NACA-WRW-92
ARR No. 4H10

NATIONAL ADVISORY COMMITTEE FOR AERONAUTICS

WARTIME REPORT

ORIGINALLY ISSUED

October 1944 as
[redacted] Report 4H10

DYNAMIC LOADS ON AIRPLANE STRUCTURES DURING LANDING

By M. A. Biot and R. L. Bisplinghoff
Bureau of Aeronautics, Navy Department

WASHINGTON

NACA ARR No. 4H10

NATIONAL ADVISORY COMMITTEE FOR AERONAUTICS

[redacted] REPORT

DYNAMIC LOADS ON AIRPLANE STRUCTURES DURING LANDING

By M. A. Biot and R. L. Bisplinghoff

1. SUMMARY

The application of transient theory to the rational determination of dynamic loads on airplane structures during initial landing impact is discussed. Simplified procedures are described by which the distribution of the maximum attainable value of the dynamic stresses in the structure may be obtained. Illustrations of the procedure are given by numerical examples for the case of airplane wings. This indicates approximate orders of magnitude to be expected in a typical problem. The validity of the underlying simplifications and assumptions is discussed. A brief outline of the general mathematical theory of transients in undamped elastic system is presented.

2. INTRODUCTION

During landing, the airplane structure undergoes transient oscillations which are excited by the initial landing impact. Recent experience has shown that in the case of large aircraft these oscillations may produce critical design conditions for the structure; whereas heretofore design loads for the landing condition have been based upon calculations which assume the structure to be rigid. Since the advent of larger aircraft has resulted in heavier and more flexible structures, these calculations are considerably in error. This together with the fact that flight load factors are reduced in the case of large aircraft makes it necessary that methods be developed for predicting dynamic landing loads. The present theoretical investigation of this problem is of a preliminary nature. It has the twofold purpose first of presenting methods by which the designer may predict the dynamic loads and second of serving as a guide in the experimental

investigation by defining the significant factors involved and determining the approximate magnitude of the quantities to be measured.

It appears that the problem may be approached in two different ways:

In the case of the landplane to consider the airplane structure and its landing gear as a whole, and to introduce the actual force displacement characteristics of the landing into the theory. In this procedure the dynamic stresses result from the sudden application of moving constraints imposed on the airplane during landing. Similarly for the seaplane the elastic structure and the water surrounding the hull may be considered as interacting bodies. While this method is not precluded in the investigation of specific cases or for research purposes, it involves inherent complexities, such as those resulting from the nonlinear properties of the landing gear and the variable-mass effects of the water surrounding the hull of a seaplane, which tends to make this type of approach less adequate for design purpose.

In the other procedure, in which stresses in the structure are considered to be caused by a landing impact force applied directly to the structure, it is assumed that the time history of the impact force may be investigated independently of the elastic properties of the structure. In this way the investigation involves two separate phases - a study of the landing forces and a study of the dynamic behavior of the structure under such forces. This procedure involves the assumption that a landing impact force may be defined in such a way that its time history is for all practical purposes independent of the elastic properties of the structure. Since it is believed that the relative simplicity of the latter approach overshadows the approximations involved, it has been adopted as the basis for the present work. This procedure was described previously in reference 1 in connection with the problem of dynamic stresses in buildings during an earthquake and the present work is essentially an adaptation to aircraft structures of the methods described in this reference.

It is assumed that in first approximation the damping and the aerodynamic forces may be neglected. The landing impact force is applied directly to the elastic structure as an external force of given time history. The response of the structure is represented as a superposition of natural modes excited by the landing impact. A first step in the

analysis is therefore to obtain the natural modes of the airplane either by calculation or by a shake test. Calculation methods have recently been developed by which natural modes of airplanes may be derived in a relatively simple way.

An important feature of the designer's approach to the landing loads problem is the fact that he is not so much interested in the actual time history of the structure as he is in the magnitude of the highest attainable stresses during the operation of the airplane. This viewpoint was introduced in the procedure by using a statistical approach. The stress amplitudes of each mode are superposed with their positive or negative values irrespective of phase and the worst possible combination is used as a basis for design. Furthermore, the stress history in each mode is not actually computed but the stress amplitude is obtained directly from a graph representing what is designated as a "dynamic response factor." This factor itself results from a statistical analysis of the effect of forces of various time histories on a single degree of freedom oscillator, using a sufficient number of such time histories to represent all possible types of landing conditions. Values of the dynamic response factors are obtained by applying typical time history excitations to a torsional pendulum (described in reference 1) and measuring the maximum amplitude of its response. In this way, when the natural modes of the airplane are known, the landing loads are readily obtained without the necessity of integrating the differential equations which govern the behavior of the elastic structure in the transient condition.

The method has its limitations and is not necessarily applicable to all types of transient problems. Some of these limitations are pointed out in the discussion, but the extent to which the methods are valid for some particular class of problems will have to be determined experimentally.

3. NOTATION

M,m	mass
k	spring constant
$Q(t)$	generalized force
ω	circular frequency

T	period
t, τ	time variable
γ	dynamic response factor
q	generalized coordinate
z	deformation displacement of any point on the wing
ϕ	normal function describing the wing mode shape
α	normal function describing the mode shape of twisting about the elastic axis
h	normal function describing the mode shape of bending of the elastic axis
I	moment of inertia
S	static mass moment
j	subscript denoting jth mode
k	subscript denoting kth spanwise wing station
ρ	mass per unit volume of prismatic beam
A	cross-sectional area of prismatic beam
E	modulus of elasticity
n	vertical landing load factor
$F(t)$	landing reaction
$N(t)$	shock strut axial force - time relation
$D(t)$	drag force - time relation caused by wheel spin-up
$a(t)$	observed acceleration time history in a drop or landing test
W	gross weight of airplane
W_L	gross weight of airplane less landing gear weight

r_e effective rolling radius of wheel

V_l landing speed

μ coefficient of sliding friction of tire on runway

s stress

I_W moment of inertia of wheel and tire about axis of rotation

T_{IN} period of shock strut axial impulse or seaplane vertical impulse

T_{ID} period of drag impulse

θ angular displacement of wheel

4. THE EVALUATION OF TRANSIENT MOTION OF ELASTIC BODIES BY THE USE OF GENERALIZED COORDINATES

As pointed out in the introduction, the theory proceeds on the assumption that the landing impact force is known. In this way the theoretical problem is reduced to the evaluation of the response of an elastic structure to a force of given time history. Methods for the determination of this landing impact force from test data will be discussed later in section 5.

In order to introduce the fundamental concepts involved in the present theory, the simplest possible elastic system will first be considered. This system is illustrated in figure 1 as a single mass oscillator.

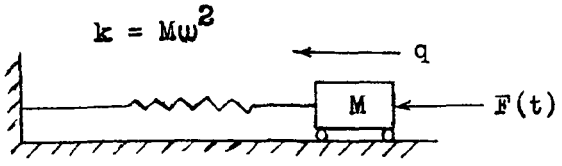

Figure 1

Denoting by M the mass and ω the natural frequency of oscillation (ω is the circular frequency expressed in radians/sec), the spring constant is $k = M\omega^2$. The expression giving the displacement q of this mass under a force $F(t)$ of arbitrary time history is well known (references 2, 3, and 4). It may be written as:

$$q = \frac{1}{M\omega}\int_0^t F(\tau) \sin \omega(t - \tau)d\tau \qquad (1)$$

where τ is a variable of integration. It is usually designated as Duhamel's integral. According to this formula the computation of the displacement q at the instant t requires the evaluation of a definite integral between the limits of integration 0 and t, and the time history of q is obtained by repeating this process for every value of t. It is noted that even in the simple case of a single-mass system the process of computing the transient response is quite elaborate. Fortunately, this difficulty may be avoided in adapting the theory to practical problems of design by considering only the maximum value of q instead of its complete time history. How this is achieved will be explained later (sec. 7).

Assume for the present that the complete time history of the deformation in the airplane structure is desired. Such a structure differs from the simple system of figure 1 by two features:

(a) It is a free body.

(b) It is an elastic body with many degrees of freedom.

In order to show how the previous discussion may be extended to include these features, consider a free system of two masses M and m connected by a spring of constant k as illustrated by figure 2.

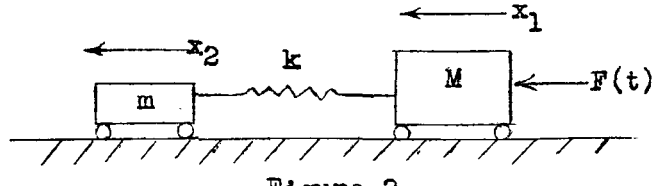

Figure 2

The mass M is under the action of a force F(t) of arbitrary time history. The straightforward way of describing the motion of this system is in terms of the displacements x_1 and x_2 of each mass. However, there is a more general approach. By an elementary analysis it is shown in appendix II that this motion may be described as the superposition of two configurations. One in which the two masses move together as a rigid body (fig. 3a), the other in which the center of gravity remains fixed with the masses moving in opposite phase and with amplitudes inversely proportional to the respective masses (fig. 3b).

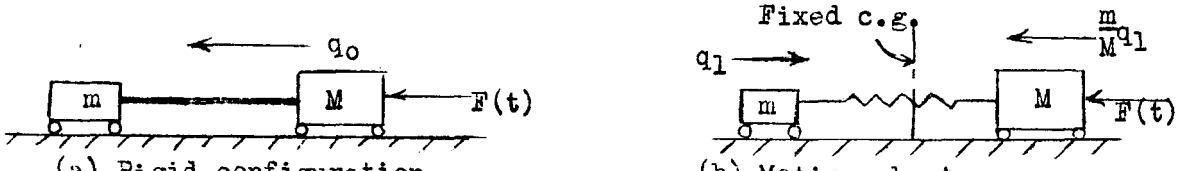

(a) Rigid configuration (b) Motion about c.g.

Figure 3

Each of these configurations has only one degree of freedom. The displacement in the first configuration is measured by the quantity q_0 and in the other by the quantity q_1. The actual displacements of the masses M and m in terms of the motion of each configuration are, respectively,

$$x_1 = q_0 + \frac{m}{M} q_1$$

$$x_2 = q_0 - q_1 \qquad (2)$$

These two configurations may be interpreted physically as representing the natural modes of oscillations of the system. From this viewpoint the rigid translation q_0 may be thought of as a mode of zero frequency or "zero mode." The other configuration where the center of gravity remains fixed and the masses move in opposite phase represents a mode of frequency ω_1. Since the coordinate q_0 of the zero mode represents the motion of the center of gravity, it is determined by the motion of a single mass $M_0 = M + m$ under the force F(t) (fig. 4a). As shown in appendix II, the motion in the mode defined by q_1 may be determined from that of an equivalent system which is constituted of a single mass M_1

elastically restrained and under the action of a force $Q_1(t)$ proportional to $F(t)$ (fig. 4b).

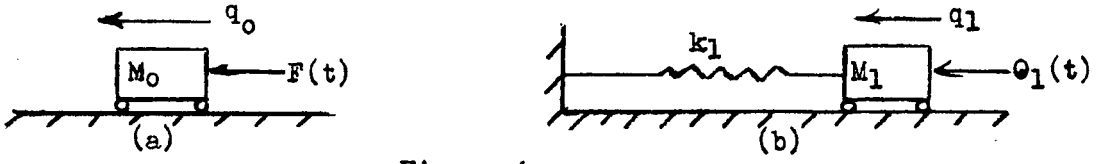

Figure 4

The natural frequency of this equivalent system is the same ω_1 as the natural frequency of the mode which it represents in the actual physical system. Such coordinates as q_0 and q_1 are called generalized coordinates. The mass M_1 of the equivalent system is referred to as the generalized mass of the corresponding mode and $Q_1(t)$ is referred to as the generalized force for this same mode. It is also shown (see appendix II) that the value of this generalized mass is derived quite simply by expressing that the kinetic energy T in the equivalent system is the same as in the corresponding mode

$$T = \frac{1}{2} M_1 \dot{q}_1^2 = \frac{1}{2} m \dot{q}_1^2 + \frac{1}{2} M \Phi^2 \dot{q}_1^2 \qquad (3)$$

where $\Phi = \frac{m}{M}$ is the ratio of the amplitudes of the masses m and M in the q_1 mode.

Hence
$$M_1 = m + M \Phi^2 \qquad (4)$$

Similarly the generalized force $Q_1(t)$ is derived by expressing that the work done by $F(t)$ on the actual system is equal to the work done by $Q_1(t)$ on the equivalent system - that is,

$$\Phi \, q_1 \, F(t) = Q_1(t) \, q_1$$

or
$$Q_1(t) = \Phi \, F(t) \qquad (5)$$

The problem of finding the transient motion of two masses connected elastically has thus been reduced to that of two independent single masses for which the motion may be expressed by Duhamel's integral (equation (1)).

Consider now a simplified airplane in which the wing is represented by two masses elastically connected to a rigid fuselage as illustrated in figure 5a.

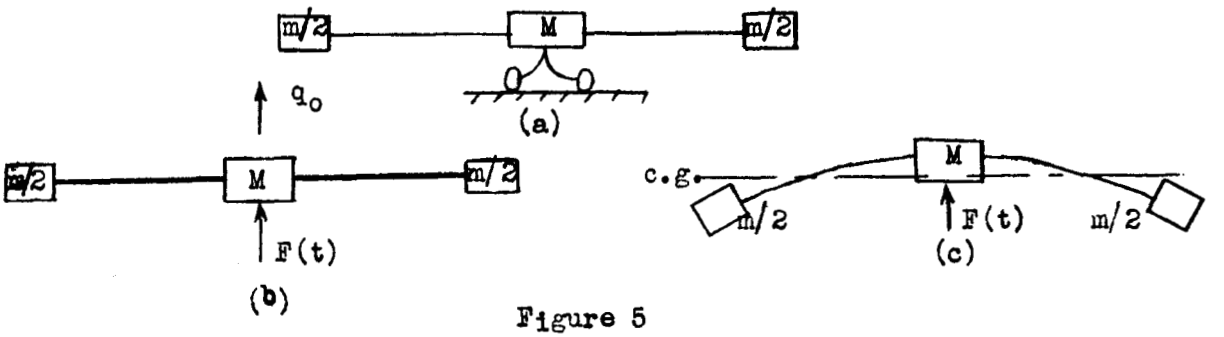

Figure 5

Obviously, for symmetric deformations this simplified structure is equivalent to the two-mass free system of figure 2. The motion under the landing impact force may be described as the superposition of a rigid translation (fig. 5b) which represents the motion of the center of gravity and a natural mode (fig. 5c) which represents the motion about the center of gravity. The equivalent single mass systems are the same as in figure 4.

This procedure may be immediately generalized to a complex airplane structure. Instead of a single deformation mode as in the case of the simplified airplane discussed above, there are actually an infinite number. It can be shown that the deformation of the structure may be represented by a superposition of these modes. If damping is neglected as is the case here, these modes are uncoupled. The behavior of each one under the landing impact force is independent of the other. The motion of each mode is represented by that of an equivalent single mass oscillator of the same natural frequency and excited by a generalized force. As an example, take the case of a wing in pure bending. There are an infinite number of bending modes, a few of which are represented in figure 6. The motion of the center of gravity represented by the rigid airplane with the generalized coordinate q_o is referred to in the present text as the "zero mode."

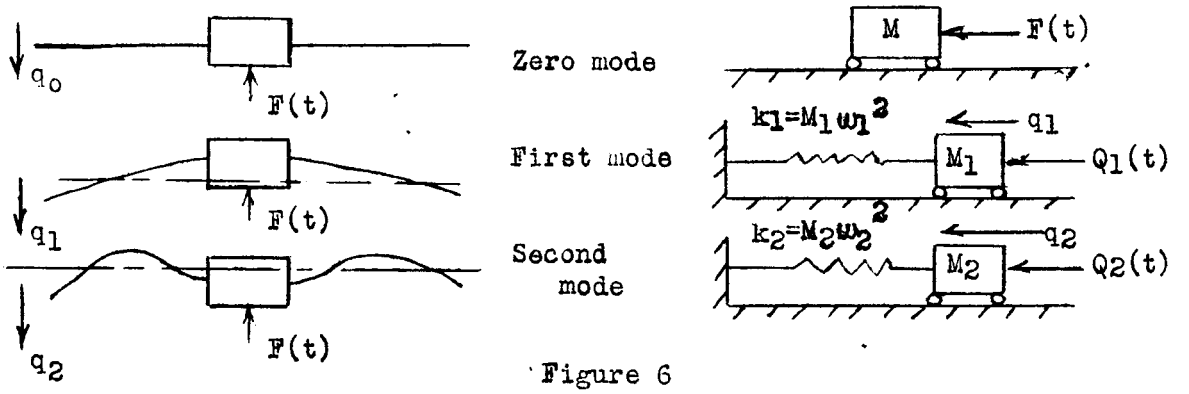

Figure 6

The amplitudes of the wing tip are usually selected as generalized coordinate and denoted by q_1 for the first mode, q_2 for the second mode, and so forth. The corresponding generalized masses are determined by the condition that the kinetic energy be the same for the mode and its equivalent system. This yields the expression:

$$M_1 = \sum_k^k \left[\phi_k^{(1)}\right]^2 m_k$$

$$M_2 = \sum_k^k \left[\phi_k^{(2)}\right]^2 m_k, \quad \text{and so forth} \tag{6}$$

In these expressions, $\phi_k^{(j)}$ represents the amplitude at station k of the mass m_k of that station in the jth mode for a unit deflection of the wing tip. Similarly, the generalized forces determined by the conditions that the work done by $F(t)$ be the same in the particular mode as the work done by $Q(t)$ in the equivalent system are

$$Q_1(t) = F(t)\,\phi_F^{(1)}$$

$$Q_2(t) = F(t)\,\phi_F^{(2)}, \quad \text{and so forth} \tag{7}$$

The subscript F refers to the station at which the landing impulse force is applied.

5. THE LANDING IMPACT FORCE F(t)

In the preceding discussion, the time history F(t) of the externally applied landing impact force is assumed to be known. In the case of a landplane, the forces are applied to the wing through an oleo strut. In the case of a flying boat, they are transmitted to the wing through a hull or pontoon.

For the landplane, a convenient source of information of axial strut characteristics is the oleo drop test. In the drop test, a mass-oleo strut system is dropped in a jig, and the acceleration time history of the mass is measured. The mass corresponds to the zero mode mass.

$$F(t) = M\, a(t) \tag{8}$$

An additional source of landing force data is from actual landings with accelerometers installed in the airplane which are capable of recording time history. This method provides the only present source of seaplane data. A sketch of such a record is shown in figure 7.

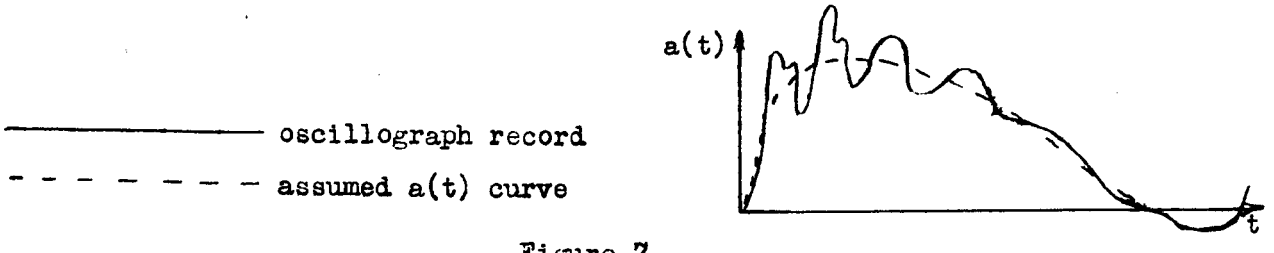

Figure 7

The high-frequency oscillations must be disregarded since they represent oscillations of the structure relative to its center of gravity. The average dotted line which is shown would be considered as a(t) in the computation of the applied landing force F(t) in equation (8).

6. EVALUATION OF THE STRESSES

Having derived the time history of the deformation of the structure, the time history of the stresses is obtained by a straightforward procedure. In this discussion, stress

is used as a general term which refers to shear or moment. It is convenient to consider the total stress as resulting from the superposition of the stresses due to the deformation in each mode. In this approach, the zero mode which is a rigid motion does not contribute any stress. Only the first mode, second mode, and so forth, have to be considered. From a practical viewpoint it is also important to note that the stresses in each mode are conveniently calculated by using the inertia forces of the natural oscillation rather than by trying to calculate the strain from the space curvature of the mode shapes. Consider, for example, a pure bending mode as represented in figure (8).

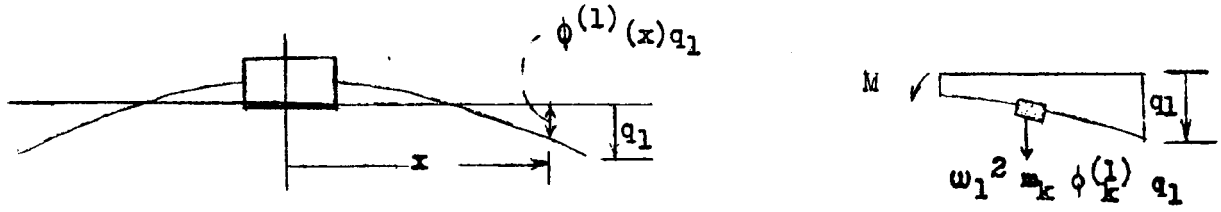

Figure 8

The shape of this mode is represented by a function $\phi^{(1)}(x)$ such that if q_1 is the tip deflection $\phi^{(1)}xq_1$ is the deflection at the location x. The bending moment in this mode is

$$M(x) = E I \frac{d^2 \phi^{(1)}(x)}{d x^2} q_1 \qquad (9)$$

M is proportional to q_1 and varies along the span as $E I \frac{d^2 \phi^{(1)}(x)}{d x^2}$. Obviously the process of computing the second derivative of $\phi^{(1)}(x)$ is elaborate and inaccurate. It is therefore preferable to derive the bending moment in each mode directly from d'Alembert's principle by expressing the equilibrium condition which exists in the natural mode between the bending moment at station k and the inertia forces $\omega_1^2 m_k \phi_k^{(1)} q_1$ due to each mass m_k located outboard from x. Similarly the shear in each mode may be obtained from the summation of all inertia forces.

It is seen that the stress $s_k^{(j)}$ in the jth mode at the kth wing station may be expressed as

$$s_k^{(j)} = A_k^{(j)} q_j \tag{10}$$

each of these stressee being proportional to the coordinate q_j of the corresponding mode. The total stress is obtained by superposition and is

$$s_k = \sum_1^j A_k^{(j)} q_j \tag{11}$$

7. THE DYNAMIC RESPONSE FACTOR V

It has been shown that the response of each mode is defined by the motion of an equivalent simple oscillator acted upon by a generalized force Q(t). The motion of a simple oscillator under the action of an arbitrary force F(t) is given by an evaluation of Duhamel's integral as shown by equation (1). Consider, for example, the motion of a simple oscillator under the influence of the isosceles triangle force-time impulse shown in figure 9.

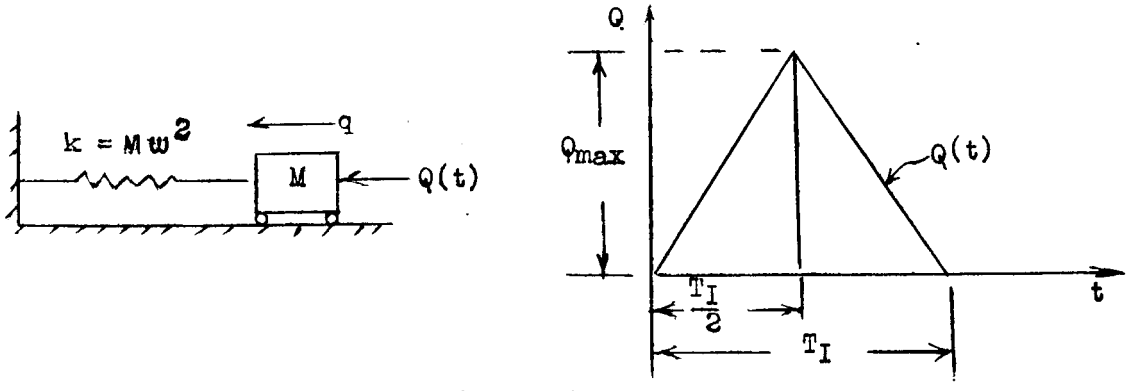

Figure 9

Let q_s = static displacement caused by Q_{max}

$T = 2\pi/\omega$ = natural period of the oscillator

T_I = period of the triangular impulse

The complete time histories of the motion of the oscillator have been evaluated for the isosceles triangular impulse for two ratios of T_I/T, and are plotted in figure 10. The response of the oscillator is expressed as a ratio of its actual displacement to its static displacement under Q_{max}.

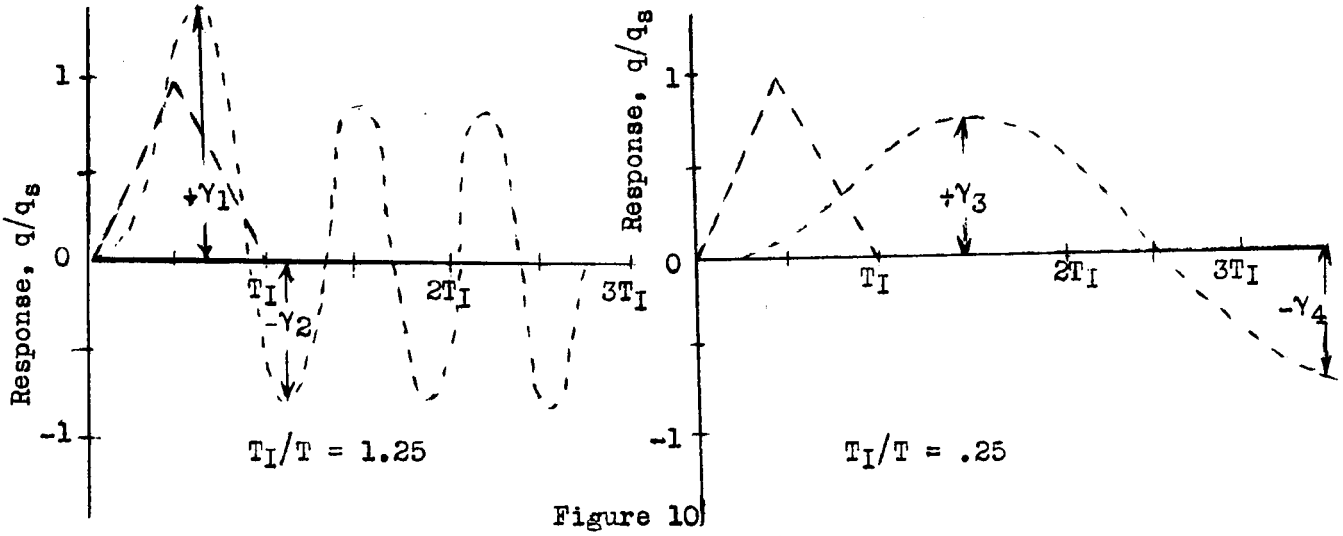

Figure 10

For each period ratio T_I/T there is a maximum value of q/q_s in the positive direction, and a maximum value in the negative direction. These maximum values are designated here as dynamic response factors and denoted by γ with the proper sign affixed. There are two values of γ associated with each period ratio as shown by figure 10. Consequently a curve may be drawn showing the variation of dynamic response factor with period ratio. Such a curve for the isosceles triangular impulse is shown by figure 11.

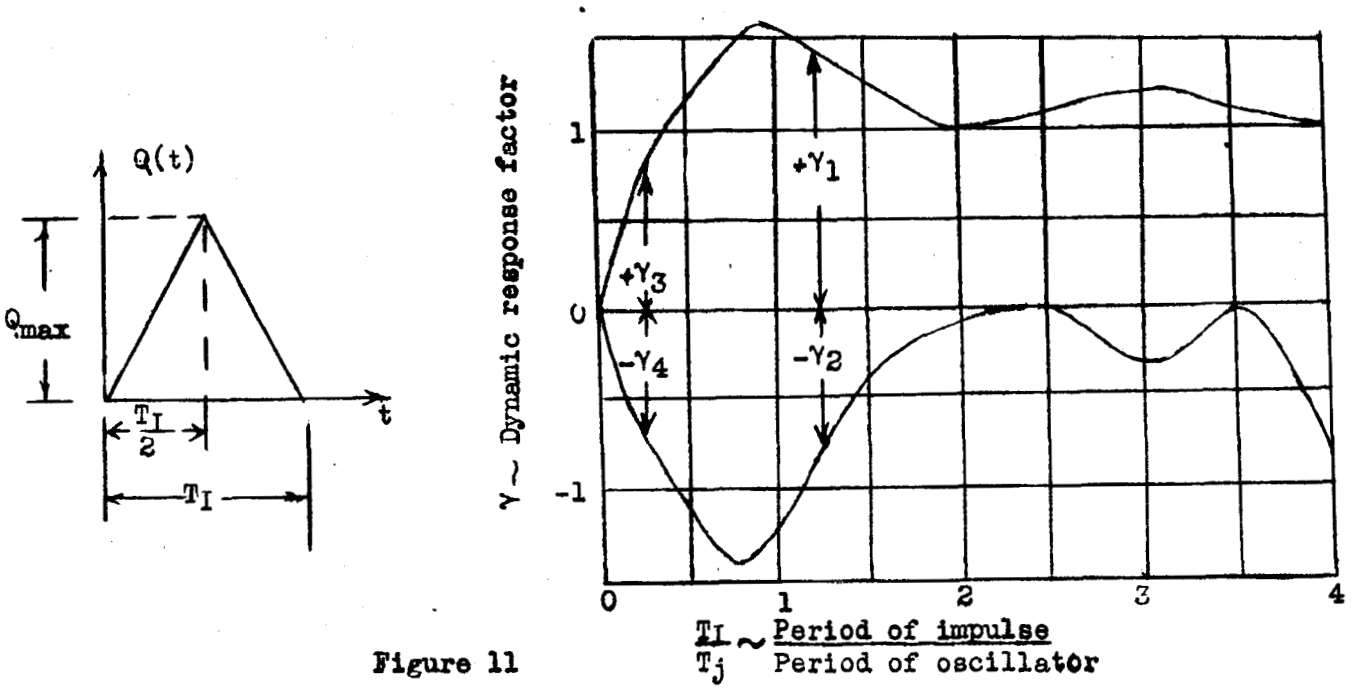

Figure 11

The determination of a dynamic response factor-period ratio curve may be accomplished for any arbitrary Q(t) variation by a numerical or analytical evaluation of Duhamel's integral. However, both processes are quite lengthy, and require plotting of the time history as shown by figure 10. A mechanical analyzer consisting of a torsional pendulum has been developed (reference 1) which may be used to measure the dynamic response factor without recourse to an evaluation of the complete time history of the motion. By such means, a dynamic response factor diagram for any shape of Q(t) curve may be evaluated in a relatively short time.

8. STATISTICAL APPROACH TO THE LANDING PROBLEM

The methods outlined above are applicable when the time history of the externally applied landing impact forces are accurately known. Actually, the shape of the landing impact force-time curve is apt to vary considerably from one landing to the next, and with different operating conditions of the airplane. Furthermore, the responses of the various modes are sensitive to small variations in the shape of the F(t) curve. For these reasons, it is not practical to design for

a single mathematical landing, but instead it is desirable to employ a statistical approach to the problem. In the previous section it was shown that the extreme positions of oscillation of a simple oscillator for any one type of applied force-time curve may be conveniently represented by means of a dynamic response factor-period ratio curve. It is possible to consider a large number of shapes of landing force-time curves varying from soft to harsh landings, and evaluate a dynamic response factor-period ratio curve for each of them. These curves may be plotted on the same graph, and an envelope curve may be drawn which bounds all of them. This envelope would represent conditions which exceed in severity every type of landing which was considered. Such a statistical basis may be used to establish design landing dynamic response factor envelopes for the landplane and the seaplane. (For example, see fig. 13.) By means of the dynamic response factor envelope, the maximum deflection of the structure in each mode during the landing may be evaluated quite simply. Considering any single mode, it is assumed that the structure is restrained to deflect in that mode only, while the maximum value of the generalized force is applied statically. The deflection may be computed under these conditions and then multiplied by the dynamic response factor in order to obtain the maximum dynamic deflection during the landing.

$$q_{j(max)} = \gamma_j \, q_{j(static)} = \gamma_j \frac{Q_{j(max)}}{M_j \, \omega_j^2} = \gamma_j \frac{F(t)_{max} \Phi^{(j)}_F}{M_j \, \omega_j^2} \qquad (12)$$

It is apparent that the phase relations between the modes are lost when an approach of this type is employed. However, this is not serious since for design purposes it must be assumed that sometime during the life of the airplane the phasing between the modes will be such as to produce the worst combination of stresses. For this reason, the maximum deflections are superposed without regard for phase in order to yield the most critical combination.

9. THE LANDPLANE WING

In the case of the landplane, the forces and moments are applied to the airplane structure through the shock

strut-tire system. These consist of a force applied in an axial direction along the shock strut caused by the landing reaction component parallel to the strut, and a moment about the landing gear attachment point caused by the landing reaction component perpendicular to the strut. Two dynamic response factors must be determined. One for the axial strut force, and one for the moment about the landing gear attachment point.

The shock strut axial force.- A study of force-time curves for axial strut reactions obtained from drop and flight test data shows that they differ considerably with pilot technique and landing attitude. A group of six types of force-time curves are considered which would represent various types of strut characteristics. These are shown in figure 12.

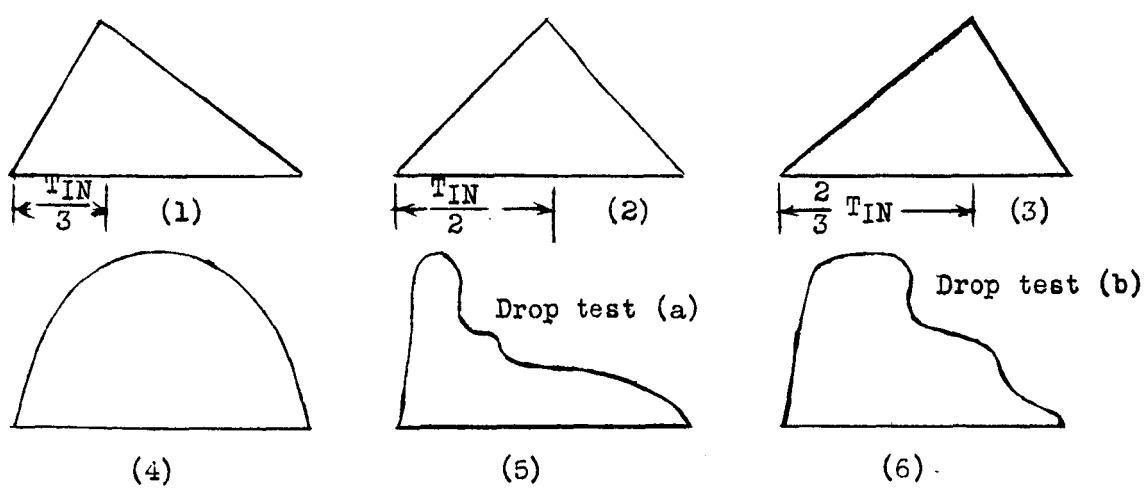

Figure 12

Dynamic response factor curves similar to figure 11 have been determined for each of these six curves by means of the mechanical analyzer (reference 1). The points which define these curves have been plotted on one graph in figure 13, and a smooth envelope curve has been drawn which bounds all of them. The condition, which the envelope shown in figure 13 represents, exceeds in severity the condition of the six types of landings considered. It is possible that after consideration of a large number of shapes of axial shock strut force-time curves taken from drop and flight test records, an envelope of this type may well represent conditions which exceed in severity every probable landing which would be experienced during the normal operation of a land-type airplane.

In order to apply the landplane dynamic response factor envelope, the impulse period must be known. A plot of limited data available at the Bureau of gross weight against landing gear vertical impulse period during the first impact of landing as determined by flight test is shown on log-log paper by figure 14. This graph has been determined from accelerometer records of various types of landings made by 11 airplanes of various weights. Each point represents an average of several landings. The equation which fits the curve drawn in figure 14 is

$$T_{IN} = 0.25 \left\{ \frac{W}{1000} \right\}^{0.1475} \tag{13}$$

where

T_{IN} axial shock strut impulse period in seconds

W gross weight of airplane in pounds

The wheel drag force.- The characteristics of the drag force on the wheel are not as well known as those of the axial strut force. The drag force is produced by the spinning up of the wheel when ground contact is made. If it is assumed that the tire is slipping or on the verge of slipping on the runway at all times during the wheel spin-up time, and that the coefficient of sliding friction μ is constant, the following differential equation may be written.

$$D(t) = \mu N(t) = \frac{I_w \ddot{\theta}}{r_e} \tag{14}$$

Integrating once gives

$$\frac{V_l I_w}{r_e^2 \mu} = \int_0^{T_{ID}} N(t)\, dt \tag{15}$$

where

V_l landing speed, feet per second

I_w moment of inertia of wheel and tire, slug-feet square

r_e effective rolling radius of wheel under impact loading, feet

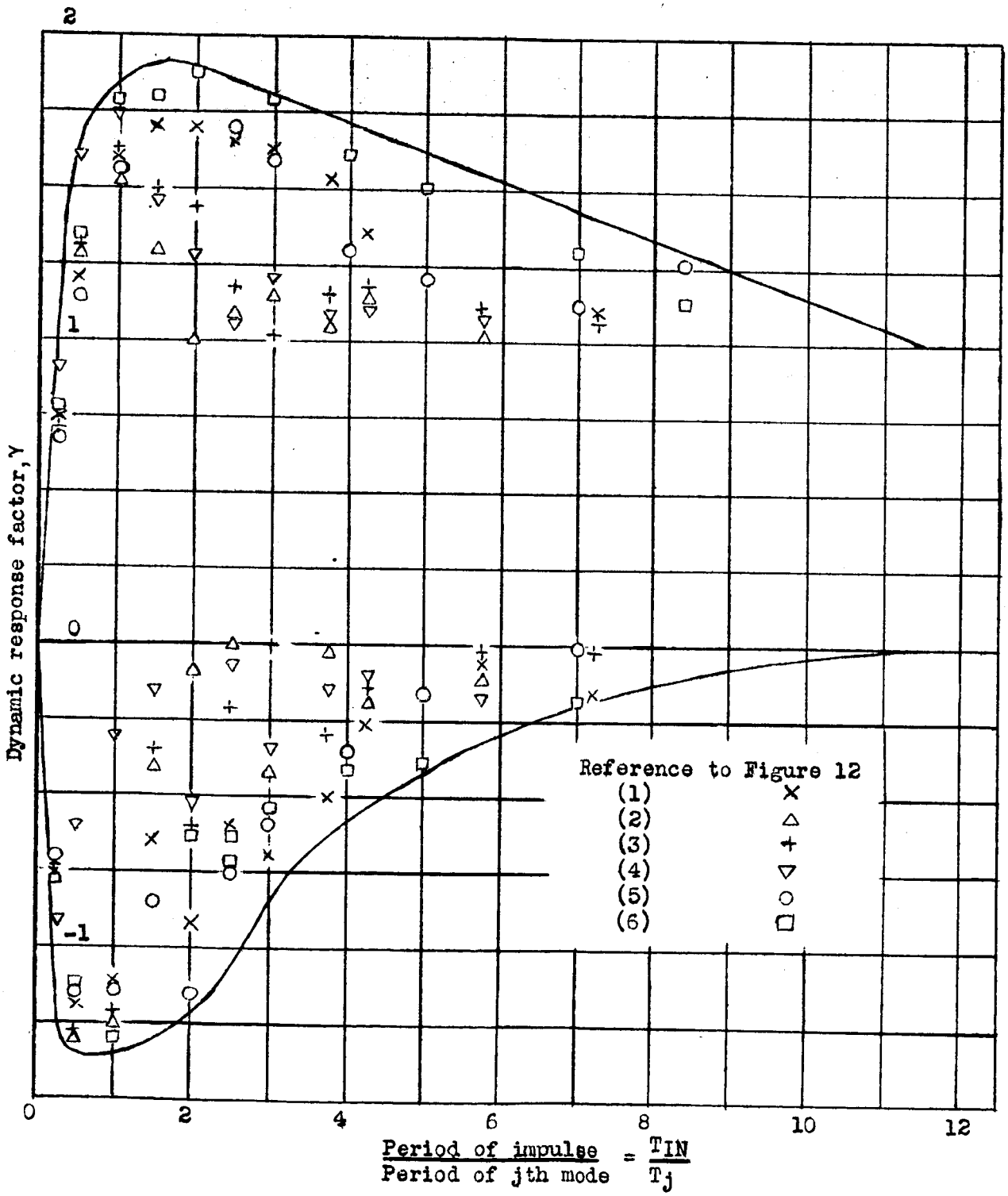

Figure 13.- Dynamic response factor envelope for landplane axial shock strut loads.

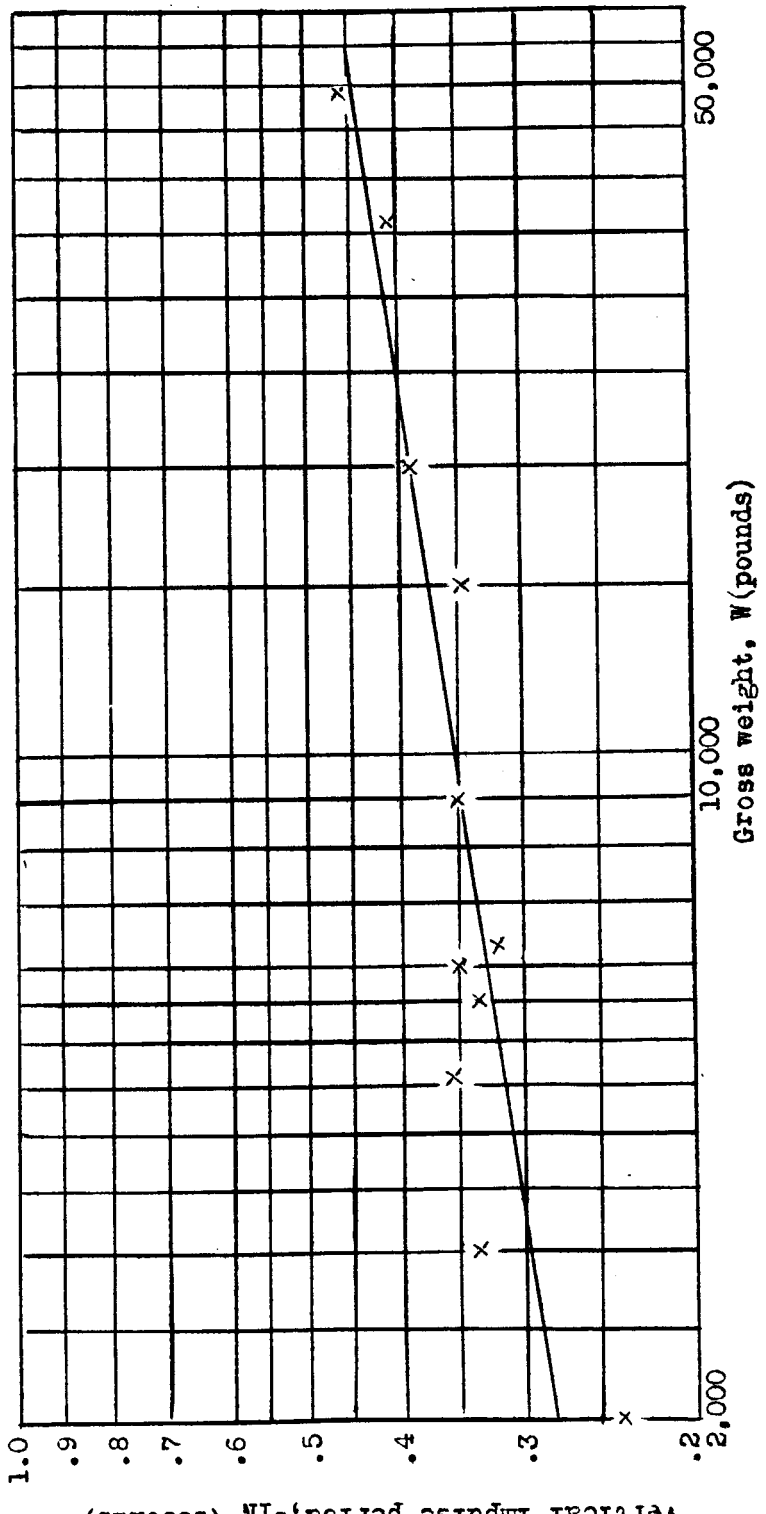

Figure 14.- Vertical impulse period during first impact of landing vs. gross weight.

T_{ID} period of drag force impulse, seconds

If the shock strut axial force is assumed to grow linearly with time during the wheel spin-up period, then equation (15) may be solved for the maximum value of the drag force in terms of the period of the drag force impulse.

$$D_{max} = \frac{2V_l I_w}{r_e^2 T_{ID}} \tag{16}$$

With the assumptions used to write equation (16), the drag force-time variation is of the type shown in figure 15.

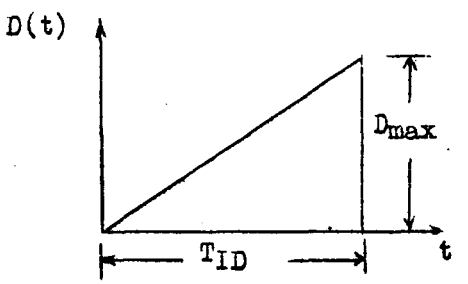

Figure 15

The dynamic response factor curve for the force-time relation shown by figure 15 is given in figure 16. The wheel spin-up time is of the order of one-fourth to one-fifth of the axial strut impulse period, and the wheel is often up to speed before the axial strut force reaches its maximum value.

In the case of modern large aircraft with retractable landing gears, the assumption that the landing gear leg is rigid in fore and aft bending may be considerably in error. Because of this lack of rigidity, there is an additional vibration mode to be considered which involves large wheel and strut amplitude and very little wing torsional motion. This lack of strut rigidity may be particularly troublesome if the fundamental fore and aft bending frequency of the landing gear is coincident with some other mode of the structure, and resonance is established.

In a general consideration of the landplane landing problem, drift and one wheel landings which excite antisymmetric wing oscillations should be considered as well as symmetric landings. The principles discussed heretofore are quite general and apply equally well in either case.

Dynamic response factor curve for landplane drag force impulse of the type shown by figure 15.

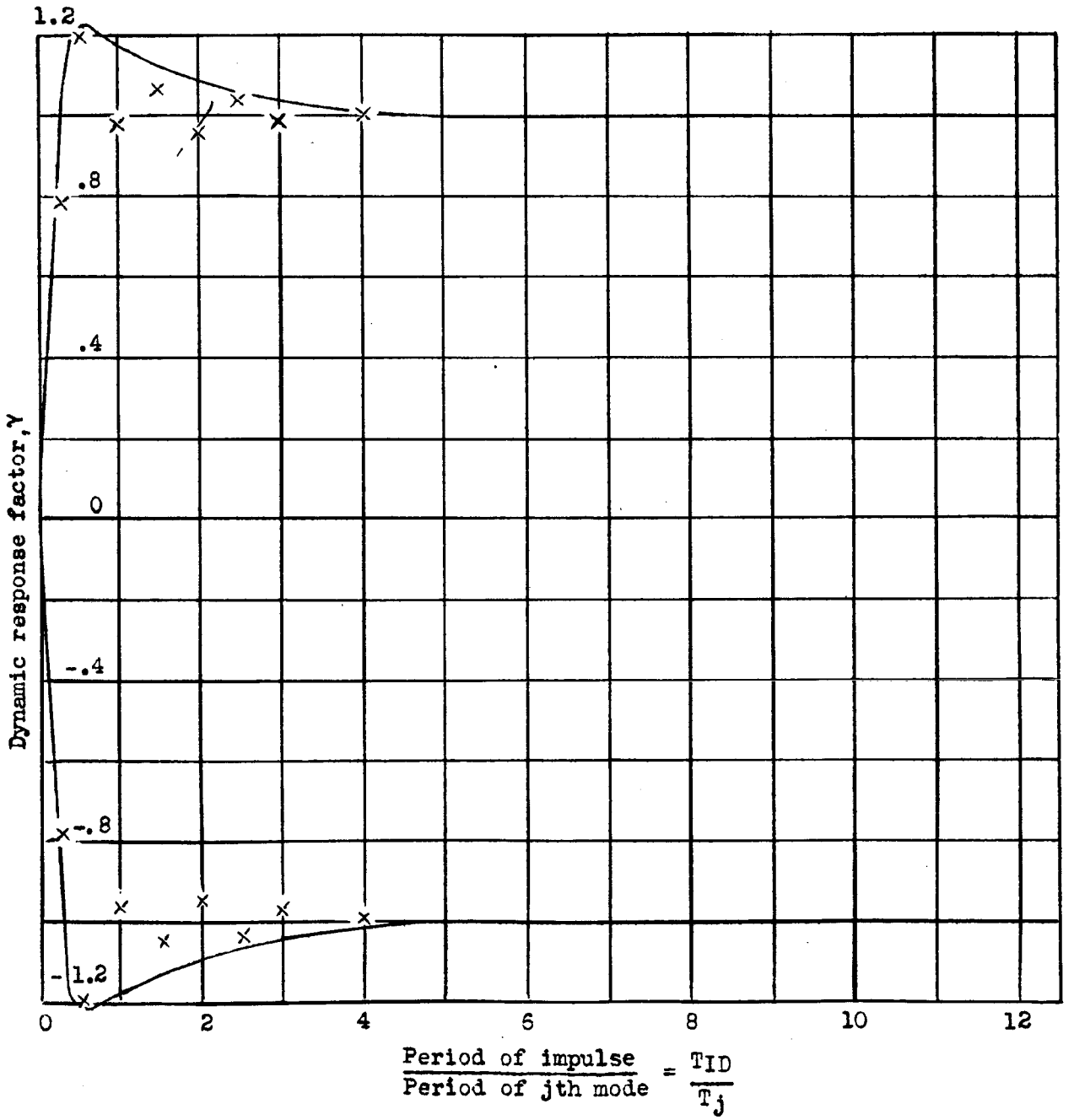

Figure 16.

10. THE FLYING BOAT WING

In the flying boat problem, the forcing impulses are transmitted to the wing through the hull structure, and the problem may be assumed identical to the landplane problem except that the force and moment is applied at the center line of the airplane rather than outboard at a landing gear station. The problem of the impact of a flying boat hull in water is considerably more complex than the landplane impact problem. A limited amount of test data is available showing time histories of center of gravity vertical and drag accelerations, and pitching acceleration for flying boats. These records indicate that the time history of the landing reaction varies widely according to landing attitude, pilot technique, condition of seaway, and detailed characteristics of hull. Theory on the seaplane impact problem is extensive; however, its applicability to the complex hull shapes of modern flying boats has not yet been demonstrated, and hence little attempt is made to use it for design purposes. Not only the force-time relations of the vertical and drag forces are necessary, but also their lines of action on the hull bottom must be known. Of these necessary items, the characteristics of the vertical force are more completely known than any of the others. Very little general information is available concerning the drag force and how the exact line of action of the vertical and drag forces vary throughout the impact period. Because of this lack of information, it is difficult to determine exactly how the impulses are applied to the flying boat wing. Furthermore, the influence of the moment on the wing vibration is undetermined unless the effect of fuselage and tail oscillations are considered. Such a consideration is beyond the scope of this discussion. A first approximation may be obtained by considering only the effect of the vertical force applied at the elastic axis of the free wing. In the absence of more complete test data it may be assumed that the vertical force on the seaplane hull, during the initial landing impact, varies as a half cycle of a sine wave. A dynamic response factor envelope has been determined for a half cycle of a sine wave impulse and is given in figure 17. The variation in the impulse period is as wide as the variation in the shape of the impulse curve, and hence it is not possible to derive an empirical relation for the impulse period from test data, as was the case with the landplane. In order to apply the dynamic response factor curve, an impulse period must be assumed, or a value taken from flight test data on an airplane

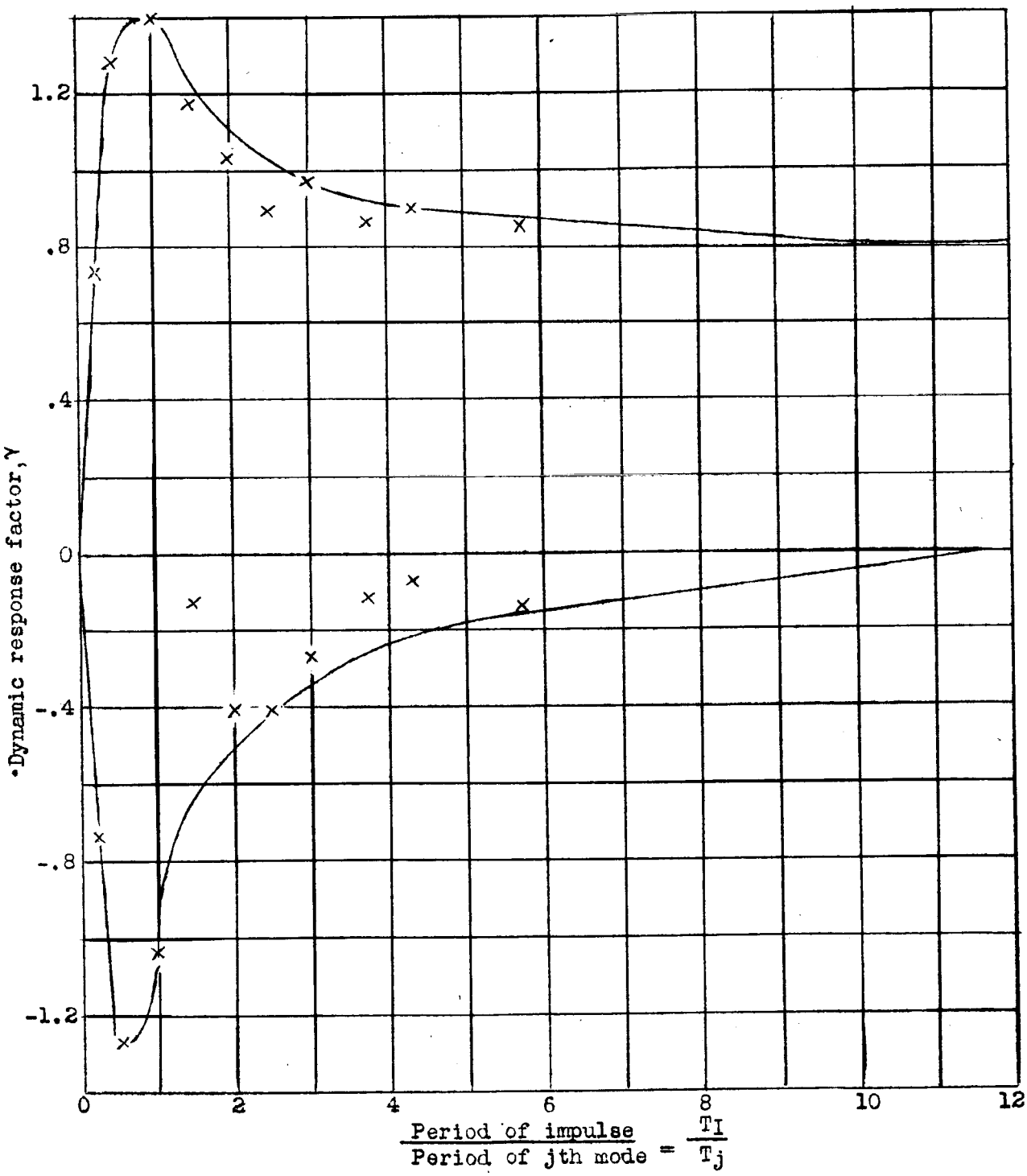

Figure 17.- Dynamic response factor curve for seaplane vertical landing force-time curve consisting of a half cycle of a sine wave.

of similar size to the one being investigated. A conservative procedure, in any case, would be to choose a period ratio T_I/T_j so as to yield the most critical combination of stresses.

11. ILLUSTRATIVE NUMERICAL EXAMPLE FOR LANDPLANE WING

The principles discussed in section 9 are illustrated by a numerical example in which the stresses due to landing in a four-engine land type bomber are computed. Mode shapes and frequencies of the free wing of this airplane were computed and transmitted in a report prepared for the Army Air Forces at C.I.T. by M. A. Biot in 1941. The bending and torsional moments are computed at seven wing stations. In this example, the wing chord is assumed parallel to the ground during the landing, and the landing gear strut is assumed to be perpendicular to the wing chord line. The landing gear strut is assumed to be rigid and rigidly attached to the wing. Figure 18 shows the assumed conditions during the landing.

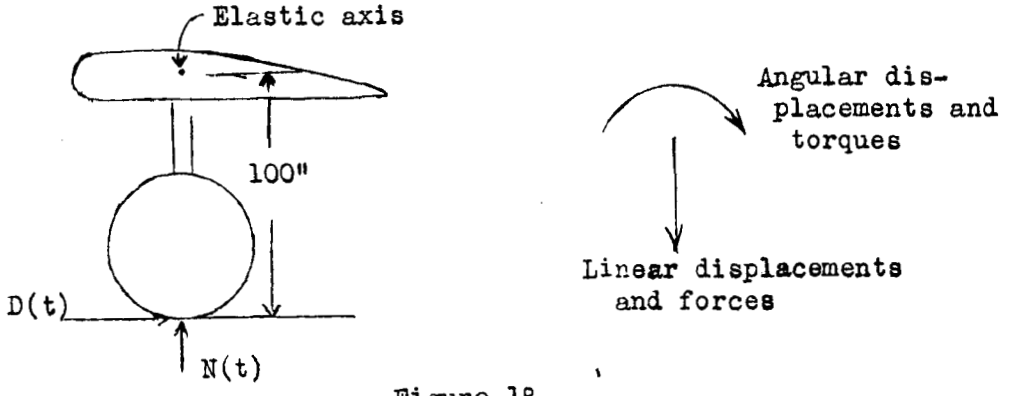

Figure 18

In this particular example, the elastic axis passes directly over the landing gear leg as is shown by figure 18. The computations may be carried out by table 1 which is self-explanatory when reference is made to appendix I. A table similar to table 1 is required for each wing mode. The mode shapes and frequencies of the free wing are taken from the Army Air Forces report prepared at C.I.T. and tabulated in tables 2, 3, and 4, where the first three wing modes are considered. The following additional data are required to complete the tables.

Gross weight, W ..... 47,200 lb
Gross weight less weight of landing gear, W_L ..... 44,426 lb
Moment of inertia of wheel and tire, I_W ..... 28 slug-ft^2
Effective rolling radius, r_e ..... 2.08 ft
Landing speed, V_s ..... 124.8 fps

From equation (13), the period of the vertical impact force is,

$$T_{IN} = 0.25 \left\{\frac{W}{1000}\right\}^{0.1475} = 0.25 \left\{\frac{47200}{1000}\right\}^{0.1475} = 0.441 \text{ second}$$

The maximum value of the vertical impact force is

$$N_{max} = \frac{1}{2} W_L n = \frac{1}{2} \times 44,426n = 22,213n$$

where n is the ultimate vertical load factor. In this example, it is assumed that $n = 4$.

$$N_{max} = (22,213)(4) = 88,852 \text{ pounds}$$

It is assumed that the period of the drag force is one-fifth that of the vertical force.

$$T_{ID} = \frac{1}{5} T_{IN} = \frac{0.441}{5} = 0.0882 \text{ second}$$

From equation (16), the maximum value of the drag force is

$$D_{max} = \frac{2V_1 I_W}{r_e^2 T_{ID}} = \frac{(2)(124.8)(28)}{(2.08)^2(0.0882)} = 18,290 \text{ pounds}$$

From the data computed in columns 5, 6, 13, and 14 in tables 2, 3, and 4, wing bending and torsional moments are plotted in figures 19 and 20, respectively, for each mode in the first and second extreme positions of oscillation. Critical values of bending moment and torsional moment at each station are obtained by adding corresponding ordinates of the three bending moment curves on the same side of the zero axis. For example, at the airplane center line, the critical negative bending moment is obtained by adding:

TABLE 1

Mode number ____ Frequency f = ____ cps

Station		m_k	S_k	I_k	h_k	α_k	$m_k h_k^2$	$I_k \alpha_k^2$	$2\alpha_k h_k S_k$
0									
1	Distance outboard from center line	Mass at station	Static mass moment about elastic axis	Moment of inertia about elastic axis	Bending deflection of elastic axis	Angular deflection about elastic axis			
2									
3									
4									
5									
6									
							a = $\sum$	b = $\sum$	c = $\sum$
							M_j = a + b + c		

See equation I-15.

	Item	Axial force	Drag moment
(1)	F_{max} or M_{max}		
(2)	M_j	Equation(I-15)	→
(3)	$\phi_F^{(j)}$	Equation(I-16)	→
(4)	T_I	Equation (13)	
(5)	T_j	1/f	1/f
(6)	T_I/T_j	(4)/(5)	(4)/(5)
(7)	$\gamma_j^{(+)}$	Figure 13	Figure 16
(8)	$\gamma_j^{(-)}$	Figure 13	Figure 16
(9)	$\eta = \frac{F_{max}\,\phi_F^{(j)}}{M_j}$	(1)×(3)/(2)	→
(10)	$\eta\gamma_j^{(+)}$	(9) × (7)	→
(11)	$\eta\gamma_j^{(-)}$	(9) × (8)	→
(12)	$a^{(+)}$ = (10) (axial) + (10) (drag)		
(13)	$a^{(-)}$ = (11) (axial) + (11) (drag)		

	(1)	(2)	(3)	(4)	(5)	(6)	(7)	(8)	(9)	(10)	(11)	(12)	(13)	(14)
Station	$a^{(+)} \times h_k$	$a^{(-)} \times h_k$	$F_k^{(+)}$ = $-m_k \times$ (1)	$F_k^{(-)}$ = $-m_k \times$ (2)	Bending moment in positive maximum position	Bending moment in negative maximum position	$a^{(+)} \times \alpha_k$	$a^{(-)} \times \alpha_k$	$T_k^{(+)}$ = $-I_k \times$ (7)	$T_k^{(-)}$ = $-I_k \times$ (8)	$\Delta T_k^{(+)}$ = $-S_k \times$ (1)	$\Delta T_k^{(-)}$ = $-S_k \times$ (2)	Total torque in positive maximum position	Total torque in negative maximum position
k = 0													(9)+(11)	(10)+(12)
k = 1														
k = 2														
k = 3														
k = 4														
k = 5														
k = 6	↓	↓	↓	↓	↓	↓	↓	↓	↓	↓	↓	↓	↓	↓

TABLE 2

Mode number 1 Frequency f = 3.365 cps

Landplane

Station		m_k	S_k	I_k	h_k	α_k	$m_k h_k^2$	$I_k \alpha_k^2$	$2\alpha_k h_k S_k$
0	0	28.5	0	∞	-0.078	0	0.1731	----------	
1	133	16.3	-640	85,234	-0.031	-0.00084	0.0157	0.0601	-0.0333
2	217	5.27	0	1,288	+0.047	-0.0016	0.01169	0.00330	
3	307	9.15	-569	61,717	+0.164	-0.00183	0.246	0.2065	+0.342
4	428	0.974	0	536	+0.374	-0.00185	0.1361	0.00184	
5	548	0.686	0	287	+0.670	-0.00187	0.308	0.0010	
6	638	0.153	0	34.1	+0.936	-0.00188	0.134	0	
							a = 1.025	b = 0.273	c = 0.309
							a + b + c = M_1 = 1.607		

	Item	Axial force	Drag moment
(1)	F_{max} or M_{max}	88,852	1,829,000
(2)	M_1	1.607	1.607
(3)	$\phi_F^{(1)}$	-0.031	-0.00084
(4)	T_I	0.441	0.088
(5)	T_1	0.297	0.297
(6)	T_I/T_1	1.485	0.296
(7)	$\gamma_1^{(+)}$	+1.90	+0.96
(8)	$\gamma_1^{(-)}$	-1.30	-0.96
(9)	$\eta = \frac{F_{max}\phi_F^1}{M_1}$	-1711	-956
(10)	$\eta\,\gamma_1^{(+)}$	-3251	-918
(11)	$\eta\,\gamma_1^{(-)}$	+2224	+918
(12)	$a^{(+)}$ = (10) (axial) + (10) (drag)		-4,169
(13)	$a^{(-)}$ = (11) (axial) + (11) (drag)		+3,142

Station	(1) $a^{(+)} \times h_k$	(2) $a^{(-)} \times h_k$	(3) $F_k^{(+)} = -m_k \times$ (1)	(4) $F_k^{(-)} = -m_k \times$ (2)	(5) Bending moment in positive maximum position	(6) Bending moment in negative maximum position	(7) $a^{(+)} \times \alpha_k$	(8) $a^{(-)} \times \alpha_k$	(9) $T_k^{(+)} = -I_k \times$ (7)	(10) $T_k^{(-)} = -I_k \times$ (8)	(11) $\Delta T_k^{(+)} = -S_k \times$ (1)	(12) $\Delta T_k^{(-)} = -S_k \times$ (2)	(13) Total torque in positive maximum position	(14) Total torque in negative maximum position
0	+326	-246	-9300	+7010	-3,940,000	+8,985,000	0	0	--------	--------			-1,092,150	+815,602
1	+129	-97	-2100	+1581	-2,719,000	+2,060,000	+3.502	-2.64	-299,000	+216,200	-+82,600	-62,100	-875,750	+661,502
2	-196	+148	+1033	-781	-1,769,000	+1,340,000	+6.68	-5.04	-8,600	+6,490			-867,150	+655,012
3	-685	+516	+6260	-4720	-844,000	+638,500	+7.64	-5.76	-471,000	+356,000	-389,500	+294,000	-6,650	+5,012
4	-1560	+1179	+1520	-1148	-356,000	+269,000	+7.72	-5.82	-4,140	+3,120			-2,510	+1,892
5	-2800	+2110	+1921	-1450	-53,850	+40,550	+7.81	-5.89	-2,242	+1,690			-268	-+202
6	-3910	+2950	+598	-451	0	0	+7.85	-5.92	-268	+202			0	0

TABLE 3

Mode number 2 **Frequency f = 4.61 cps**

Landplane

Station		m_k	S_k	I_k	h_k	α_k	$m_k h_k^2$	$I_k \alpha_k^2$	$2\alpha_k h_k S_k$
0	0	28.5	0	∞	-0.1237	0	0.436	———	
1	133	16.3	-640	85,234	-0.0693	+0.0057	0.0783	2.77	+0.505
2	217	5.27	0	1,288	+0.0330	+0.0073	0.0058	.0685	
3	307	9.15	-569	61,717	+0.229	+0.0095	0.480	5.57	-2.48
4	428	0.974	0	536	+0.756	-0.00956	0.556	0.0491	
5	548	0.686	0	387	+1.741	-0.00964	2.085	0.0266	
6	638	0.153	0	34.1	+2.862	-0.00868	1.273	0.0032	
							a = 4.914	b = 8.488	c = -1.975
							a + b + c = M_2 = +11.427		

	Item	Axial force	Drag moment
(1)	F_{max} or M_{max}	88,852	1,829,000
(2)	M_2	11.427	11.427
(3)	$\phi_F^{(2)}$	-0.0693	+0.0057
(4)	T_I	0.441	0.088
(5)	T_2	0.2165	0.2165
(6)	T_I/T_2	2.04	0.406
(7)	$\gamma_2^{(+)}$	+1.90	+1.80
(8)	$\gamma_2^{(-)}$	-1.80	-1.80
(9)	$\eta = \frac{F_{max}\phi_F^{(2)}}{M_2}$	-537	+911
(10)	$\eta\,\gamma_2^{(+)}$	-1020	+1093
(11)	$\eta\,\gamma_2^{(-)}$	+644	-1093
(12)	$a^{(+)}$ = (10) (axial) + (10) (drag)		+73
(13)	$a^{(-)}$ = (11) (axial) + (11) (drag)		-449

	(1)	(2)	(3)	(4)	(5)	(6)	(7)	(8)	(9)	(10)	(11)	(12)	(13)	(14)
Station	$a^{(+)} \times h_k$	$a^{(-)} \times h_k$	$F_k^{(+)} = -m_k \times$ (1)	$F_k^{(-)} = -m_k \times$ (2)	Bending moment in positive maximum position	Bending moment in negative maximum position	$a^{(+)} \times \alpha_k$	$a^{(-)} \times \alpha_k$	$T_k^{(+)} = -I_k \times$ (7)	$T_k^{(-)} = -I_k \times$ (8)	$\Delta T_k^{(+)} = -S_k \times$ (1)	$\Delta T_k^{(-)} = -S_k \times$ (2)	Total torque in positive maximum position	Total torque in negative maximum position
0	-9.04	+55.5	+258	-1581	+92,400	-790,000	0	0	---------	---------			-73,316	+450,909
1	-5.06	+31.1	+82.5	-506.5	+68,300	-583,000	+0.416	-2.56	-35,500	+218,100	-3240	+19,900	-34,576	+212,909
2	+2.41	-14.8	-12.71	+78	+48,100	-411,000	+0.533	-3.28	-686	+4,220			-33,890	+208,689
3	+16.71	-102.9	-153	+941	+27,190	-232,500	+0.694	-4.26	-42,800	+363,500	+9510	-58,500	-600	+3,689
4	+55.2	-340	-53.8	+331	+12,290	-105,000	+0.698	-4.29	-374	+2,300			-226	+1,389
5	+127.1	-782	-87.4	+537	+2,905	-17,810	+0.704	-4.32	-202	+1,241			-24.1	+148
6	+211	-1295	-32.3	+198	0	0	+0.706	-4.34	-24.1	+148			0	0

TABLE 4

Mode number 3 — Frequency f = 8.46 cps

Landplane

Station		m_k	S_k	I_k	h_k	α_k	$m_k h_k^2$	$I_k \alpha_k^2$	$2\alpha_k h_k S_k$
0	0	28.5	0	∞	+0.0426	0	0.0519	---------	
1	133	16.3	-640	85,234	-0.0064	-0.00213	0.000668	0.386	-0.0175
2	217	5.27	0	1,288	-0.0710	-0.00132	0.0266	0.00224	
3	307	9.15	-569	61,717	-0.1250	-0.00018	0.1430	0.002	-0.0256
4	428	0.974	0	536	-0.0370	-0.00014	0.0013	0.00001052	
5	548	0.686	0	287	+0.3890	-0.00010	0.104	0.000003	
6	638	0.153	0	34.1	+1.045	-0.00008	0.167	0	
							a = 0.494	b = 0.390	c = -0.0431
							a + b + c = M_3 = +0.841		

	Item	Axial force	Drag moment
(1)	F_{max} or M_{max}	88,852	1,829,000
(2)	M_3	0.841	0.841
(3)	$\phi_F^{(3)}$	-0.0064	-0.00213
(4)	T_I	0.441	0.088
(5)	T_3	0.118	0.118
(6)	T_I/T_3	3.74	0.745
(7)	$\gamma_3^{(+)}$	+1.73	+1.21
(8)	$\gamma_3^{(-)}$	-0.63	-1.21
(9)	$\eta = \frac{F_{max}\,\phi_F^3}{M_3}$	-675	-463
(10)	$\eta\,\gamma_3^{(+)}$	-1168	-560
(11)	$\eta\,\gamma_3^{(-)}$	+425	+560
(12)	$a^{(+)}$ = (10) (axial) + (10) (drag)	-1728	
(13)	$a^{(-)}$ = (11) (axial) + (11) (drag)	+985	

	(1)	(2)	(3)	(4)	(5)	(6)	(7)	(8)	(9)	(10)	(11)	(12)	(13)	(14)
Station	$a^{(+)} \times h_k$	$a^{(-)} \times h_k$	$F_k^{(+)} = -m_k \times$ (1)	$F_k^{(-)} = -m_k \times$ (2)	Bending moment in positive maximum position	Bending moment in negative maximum position	$a^{(+)} \times \alpha_k$	$a^{(-)} \times \alpha_k$	$T_k^{(+)} = -I_k \times$ (7)	$T_k^{(-)} = -I_k \times$ (8)	$\Delta T_k^{(+)} = -S_k \times$ (1)	$\Delta T_k^{(-)} = -S_k \times$ (2)	Total torque in positive maximum position	Total torque in negative maximum position
0	-73.6	+42	+2100	-1198	+372,000	212,200	0	0	---------	---------			-142,525	+117,587
1	+110.7	-6.3	-1802	+102.9	+87 900	-49,850	+3.68	-2.1	-314,000	+179,000	+70,900	-4,040	+100,575	-57,373
2	+122.9	-70	-648	+369	-77,000	+43,700	+2.28	-1.30	-2,940	+1,672			+103,515	-59,045
3	+216	-123.1	-1977	+1129	-195,000	+110,900	+0.311	-0.1771	-19,200	+10,950	+122,900	-70,100	-184.32	+104.99
4	+63.9	-36.4	-62.2	+35.4	-113,200	+64,400	+0.242	-0.138	-130	+74.1			-54.32	+30.89
5	-671	+383	+461	-263	-24,950	+14,190	+0.1728	-0.0985	-49.6	+28.2			-4.72	+2.69
6	-1809	+1030	+276.5	-157.5	0	0	+0.1381	-0.0789	-4.72	+2.69			0	0

	Inch-pounds
First mode - positive maximum	-3,940,000
Second mode - negative maximum	-790,000
Third mode - negative maximum	-212,000
Maximum negative bending moment at the center line =	-4,942,000

Similarly, for the maximum negative torsional moment at the center line, the following are added:

	Inch-pounds
First mode - positive maximum	-1,092,150
Second mode - positive maximum	-73,316
Third mode - positive maximum	-142,525
Maximum negative torsional moment at the center line =	-1,307,991

The frequency of the fourth mode is approximately 1350 cpm, and hence its contribution to the stress would be small. This is true because of the tendency for $\phi_F^{(j)}$ to be reduced to small values in the higher modes, and because of the inhibitive effect which the aerodynamic and structural damping has upon the higher modes. It is important to remember that the stresses, shown here must be superposed upon the steady stresses produced by the aerodynamic loads on the wing during landing.

12. ILLUSTRATIVE NUMERICAL EXAMPLE FOR SEAPLANE WING

The principles discussed for the seaplane are illustrated by a numerical example. In this example, a four-engine land type patrol bomber is considered as being a flying boat in order that the same mode shapes and frequencies may be used. The bending and torsional moments are computed at seven wing stations for a vertical load factor of 1, and the effect of the drag force is neglected. The first three deformation modes of the free wing are considered, and the computations are carried out by means of table 1. The vertical force on the hull is assumed perpendicular to the wing chord during impact.

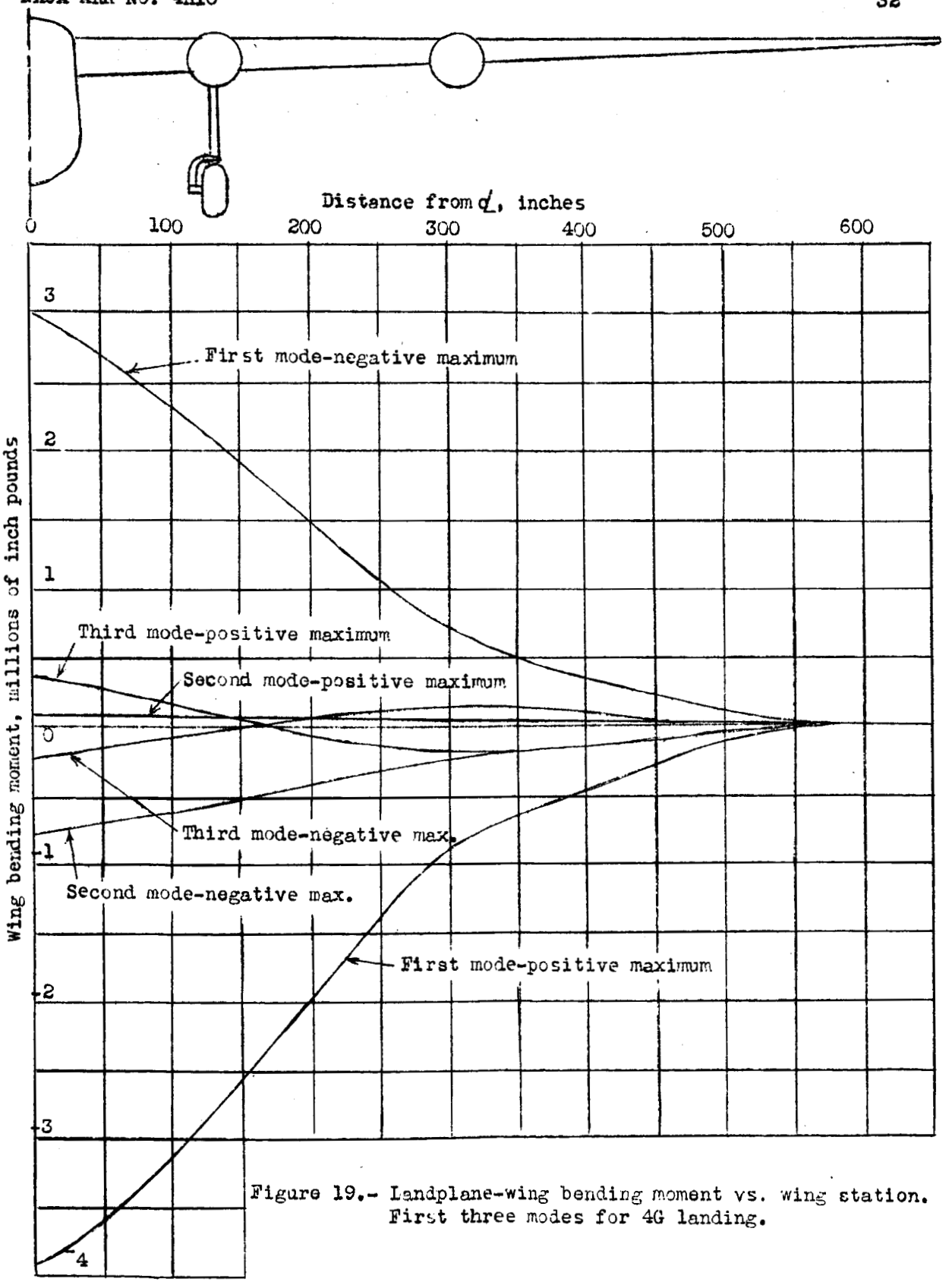

Figure 19.- Landplane-wing bending moment vs. wing station. First three modes for 4G landing.

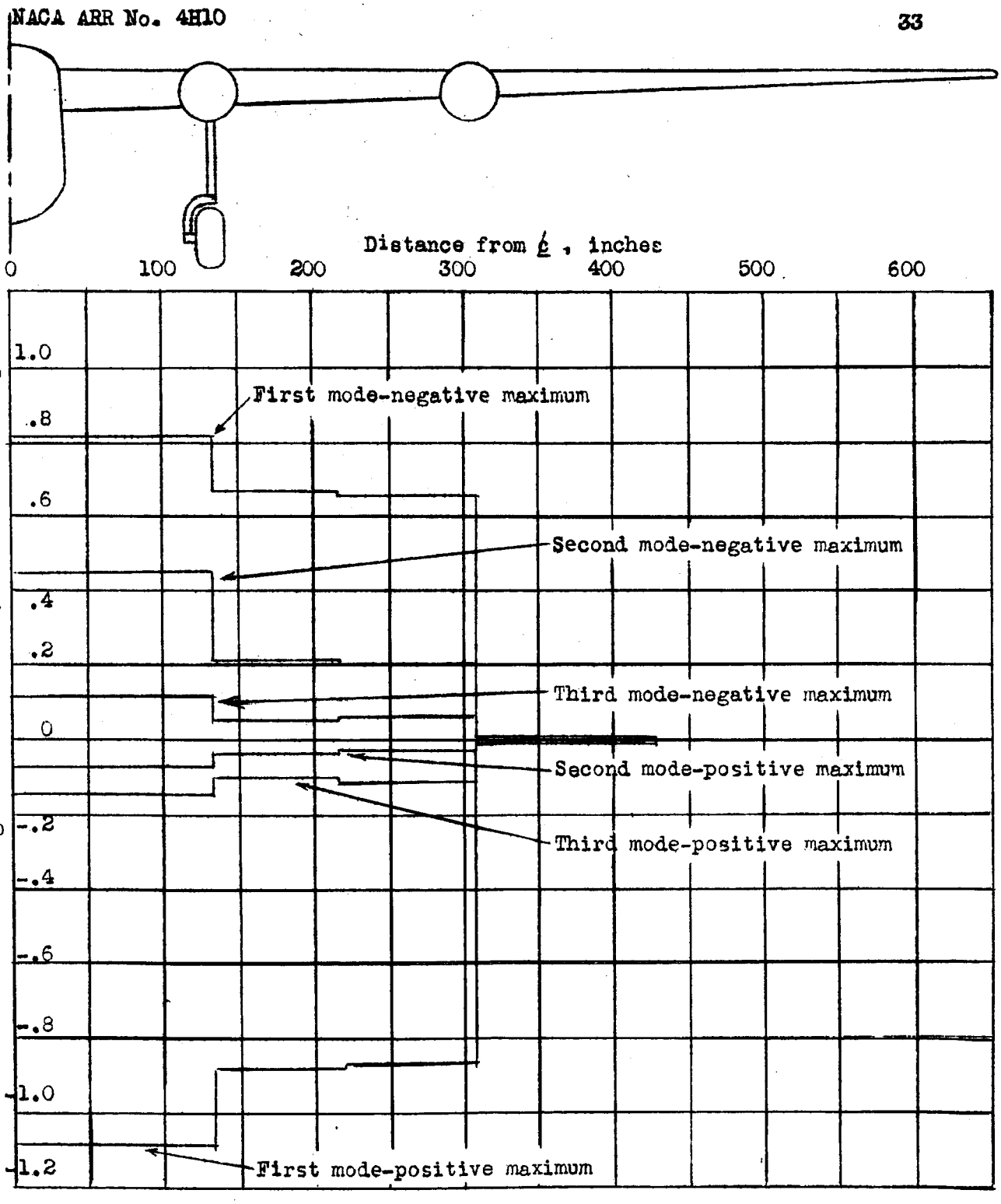

Figure 20.- Landplane-wing torsional moment vs. wing station. First three modes for 4G landing.

The following sketch shows the assumed conditions during the landing.

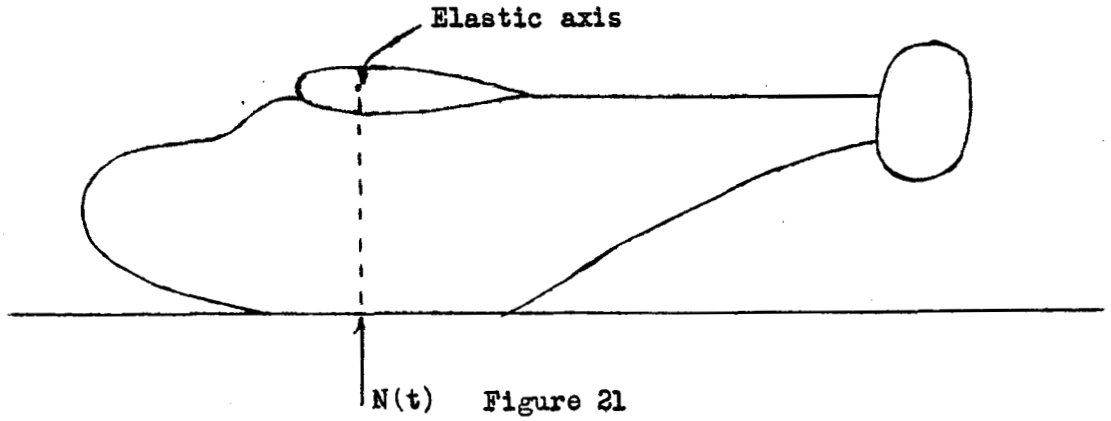

Figure 21

For purpose of this example, an impulse period of 0.2 second is arbitrarily assumed. From the data computed in columns 5, 6, 13, and 14 in tables 5, 6, and 7, wing bending and torsional moments are plotted in figures 22 and 23, respectively, for each mode in the first and second extreme positions of oscillation for a vertical load factor of 4. The values plotted in figures 22 and 23 are four times the value s shown in columns 5, 6, 13, and 14 in tables 5, 6, and 7.

13. DISCUSSION

In the usual landing with large aircraft there is a period of initial impact followed by a short interval during which the airplane is airborne. It is to conditions existing during the initial impact and shortly thereafter that the present theory of transients is applicable. In the ensuing motion during run-out, the wheels are substantially in contact with the ground or the hull with the water. During this latter phase of the motion, the structure has imposed upon it a series of alternating loads depending upon the ground contour or the condition of the seaway. It may be possible that a resonance condition during the latter phase of the landing may produce stresses more critical than those produced during and shortly after the initial impact.

A preliminary analytical investigation into the effect of aerodynamic damping has shown that it may be neglected with small error; however, this is subject to experimental

TABLE 5

Mode number 1 Frequency f = 3.365 cps

Flying boat

Station		m_k	S_k	I_k	h_k	α_k	$m_k h_k^2$	$I_k \alpha_k^2$	$2\alpha_k h_k S_k$
0	0	28.5	0	∞	-0.078	0	0.1731	----------	
1	133	16.3	-640	85,234	-0.031	-0.00084	0.0157	0.0601	-0.0333
2	217	5.27	0	1,288	+0.047	-0.0016	0.01169	0.0033	
3	307	9.15	-569	61,717	+0.164	-0.00183	0.246	0.2065	+0.342
4	428	0.974	0	536	+0.374	-0.00185	0.1361	0.00184	
5	548	0.686	0	287	+0.670	-0.00187	0.308	0.0010	
6	638	0.153	0	34.1	+0.936	-0.00188	0.134	0	
							a = 1.025	b = 0.273	c = 0.309
							a + b + c = M_1 = 1.607		

Item		Vertical force
(1)	F_{max}	23,600
(2)	M_1	1.607
(3)	$\phi_F^{(1)}$	-0.078
(4)	T_I	0.200
(5)	T_1	0.297
(6)	T_I/T_1	0.674
(7)	$\gamma_1^{(+)}$	+1.72
(8)	$\gamma_1^{(-)}$	-1.57
(9)	$\eta = \frac{F_{max}\phi_F^1}{M_1}$	-1,147
(10)	$\eta x \gamma_1^{(+)}$	-1,973
(11)	$\eta x \gamma_1^{(-)}$	+1,801

	(1)	(2)	(3)	(4)	(5)	(6)	(7)	(8)	(9)	(10)	(11)	(12)	(13)	(14)
Station	$\eta x \gamma_1^{(+)} x h_k$	$\eta x \gamma_1^{(-)} x h_k$	$F_k^{(+)} = -m_k x$ (1)	$F_k^{(-)} = -m_k x$ (2)	Bending moment in positive maximum position	Bending moment in negative maximum position	$\eta x \gamma_1^{(+)} x \alpha_k$	$\eta x \gamma_1^{(-)} x \alpha_k$	$T_k^{(+)} = -I_k x$ (7)	$T_k^{(-)} = -I_k x$ (8)	$\Delta T_k^{(+)} = -S_k x$ (1)	$\Delta T_k^{(-)} = -S_k x$ (2)	Total torque in positive maximum position	Total torque in negative maximum position
0	+154	-140.9	-4390	+4010	-1,870,000	+1,709,000	0	0	---------	---------			-516,305	+471,779
1	+61.2	-55.9	-999	+911	-1,288,000	+1,172,000	+1.66	-1.51	-141,700	+128,900	+39,200	-35,800	-413,805	+378,679
2	-92.9	+84.6	+489	-446	-836,400	+264,000	+3.16	-2.88	-4,060	+3,705			-409,745	+374,974
3	-324	+296	+2962	-2705	-398,800	+364,400	+3.61	-3.30	-222,500	+204,000	-184,100	+168,100	-3,145	+2,874
4	-739	+674	+720	-656	-168,200	+153,700	+3.65	-3.34	-1,959	+1,791			-1,186	+1,083
5	-1321	+1209	+908	-830	-25,400	+23,200	+3.69	-3.37	-1,060	+ 967			-126	+116
6	-1850	+1690	+283	-258	0	0	+3.71	-3.39	-126.5	+115.7			0	0

TABLE 8

Deformation mode number 2 **Frequency f = 4.61 cps**

Seaplane

Station		m_k	S_k	I_k	h_k	α_k	$m_k h_k^2$	$I_k \alpha_k^2$	$2\alpha_k h_k S_k$
0	0	28.5	0	∞	-0.1237	0	0.436	----------	0
1	133	16.3	-640	85,234	-0.0693	+0.0057	0.0783	2.77	+0.505
2	217	5.27	0	1,288	+0.0330	+0.0073	0.0058	0.0685	0
3	307	9.15	-569	61,717	+0.229	+0.0095	0.480	5.57	-2.48
4	428	0.974	0	536	+0.756	+0.00956	0.556	0.0491	0
5	548	0.686	0	287	+1.741	+0.00964	2.085	0.0266	0
6	638	0.153	0	34.1	+2.882	+0.00968	1.273	0.0032	0
							a = 4.914	b = 8.488	c = -1.975
							a + b + c = M_2 = 11.427		

Item		Vertical force
(1)	F_{max}	23,600
(2)	M_2	11.427
(3)	$\phi_F^{(2)}$	-0.1237
(4)	T_I	0.200
(5)	T_2	0.2165
(6)	T_I/T_2	0.923
(7)	$\gamma_2^{(+)}$	+1.75
(8)	$\gamma_2^{(-)}$	-1.45
(9)	$\eta = \frac{F_{max}\,\phi_F^2}{M_2}$	-255.5
(10)	$\eta\,\gamma_2^{(+)}$	-447
(11)	$\eta\,\gamma_2^{(-)}$	+370

	(1)	(2)	(3)	(4)	(5)	(6)	(7)	(8)	(9)	(10)	(11)	(12)	(13)	(14)
Station	$\eta \times \gamma_2^{(+)} \times h_k$	$\eta \times \gamma_2^{(-)} \times h_k$	$F_k^{(+)} = -m_k \times$ (1)	$F_k^{(-)} = -m_k \times$ (2)	Bending moment in positive maximum position	Bending moment in negative maximum position	$\eta \times \gamma_2^{(+)} \times \alpha_k$	$\eta \times \gamma_2^{(-)} \times \alpha_k$	$T_k^{(+)} = -I_k \times$ (7)	$T_k^{(-)} = -I_k \times$ (8)	$\Delta T_k^{(+)} = -S_k \times$ (1)	$\Delta T_k^{(-)} = -S_k \times$ (2)	Total torque in positive maximum position	Total torque in negative maximum position
0	+55.4	-45.8	-1580	+1305	-796,000	+658,000	0	0	--------	--------			+448,893	-372,208
1	+31.0	-25.6	-505	+417	-589,000	+485,000	-2.55	+2.11	+217,500	-180,000	+19,820	-16,390	+211,573	-175,818
2	-14.8	+12.2	+78.1	-64.4	-414,000	+342,000	-3.26	+2.70	+4,190	-3,475			+207,383	-172,343
3	-102.5	+84.8	+934	-776	-234,000	+193,500	-4.25	+3.52	+262,100	-217,500	-58,400	+48,200	+3,683	-3,043
4	-338	+280	+329	-272	-105,900	+87,200	-4.28	+3.54	+2,297	-1,900			+1,386	-1,143
5	-780	+645	+535	-442	-17,910	+14,810	-4.31	+3.56	+1,239	-1,021			+147	-122
6	-1291	+1069	+197	-163	0	0	-4.33	+3.58	+147	-122			0	0

TABLE 7

Deformation mode number 3 Frequency $f = 8.46$ cps

Seaplane

Station		m_k	s_k	I_k	h_k	α_k	$m_k h_k^2$	$I_k \alpha_k^2$	$\Sigma \alpha_k h_k s_k$
0	0	28.5	0	∞	+0.0426	0	0.0519	----------	0
1	133	16.3	-640	85,234	-0.0064	-0.00213	0.000668	0.386	-0.0175
2	217	5.27	0	1,288	-0.0710	-0.00132	0.0266	0.00224	0
3	307	9.15	-569	61,717	-0.1350	-0.00018	0.1430	0.002	-0.0256
4	428	0.974	0	536	-0.0370	-0.00014	0.0013	0.0000105	0
5	548	0.686	0	287	+0.3890	-0.00010	0.104	0.000003	0
6	638	0.153	0	34.1	+1.045	-0.00008	0.167	0	0
							a = 0.494	b = 0.390	c = -0.0431
							a + b + c = M_3 = 0.841		

Item		Vertical force
①	F_{max}	23,600
②	M_3	0.841
③	$\phi_F^{(3)}$	+0.0426
④	T_I	0.200
⑤	T_3	0.118
⑥	T_I/T_3	1.695
⑦	$\gamma_3^{(+)}$	+1.475
⑧	$\gamma_3^{(-)}$	-0.725
⑨	$\eta = \frac{F_{max}\,\phi_F^3}{M_3}$	+1197
⑩	$\eta\,\gamma_3^{(+)}$	+1766
⑪	$\eta\,\gamma_3^{(-)}$	-868

	①	②	③	④	⑤	⑥	⑦	⑧	⑨	⑩	⑪	⑫	⑬	⑭
Station	$\eta \times \gamma_3^{(+)} \times h_k$	$\eta \times \phi_3^{(-)} \times h_k$	$F_k^{(+)} = -m_k \times$ ①	$F_k^{(-)} = -m_k \times$ ②	Bending moment in positive maximum position	Bending moment in negative maximum position	$\eta \times \gamma_3^{(+)} \times \alpha_k$	$\eta \times \gamma_3^{(-)} \times \alpha_k$	$T_k^{(+)} = -I_k \times$ ⑦	$T_k^{(-)} = -I_k \times$ ⑧	$\Delta T_k^{(+)} = -s_k \times$ ①	$\Delta T_k^{(-)} = -s_k \times$ ②	Total torque in positive maximum position	Total torque in negative maximum position
0	+75.4	-37	-2145	+1055	-381,000	+187,000	0	0	----------				+210,569	-103,851
1	-11.3	+5.55	+184	-90.5	-89,300	+44,100	-3.76	+1.85	+320,500	-157,900	-7,340	+3,555	-108,691	+50,494
2	-125.3	+61.6	+661	-325	+78,400	-38,700	-2.33	+1.145	+3,000	-1,474			-105,691	+51,968
3	-220.6	-108.3	+2020	-993	+198,800	-98,000	-0.318	+0.156	+19,620	-9,640	-125,500	+61,700	+189	-92
4	-65.4	-32.1	+63.6	-31.2	+115,300	-57,000	-0.247	+0.121	+133	-65			+56	-27
5	+686	-338	-471	+232	+25,400	-12,520	-0.177	+0.087	+51	-25			+5	-2
6	+1849	-907	-283	+139	0	0	-0.141	+0.069	+4.81	-2.36			0	0

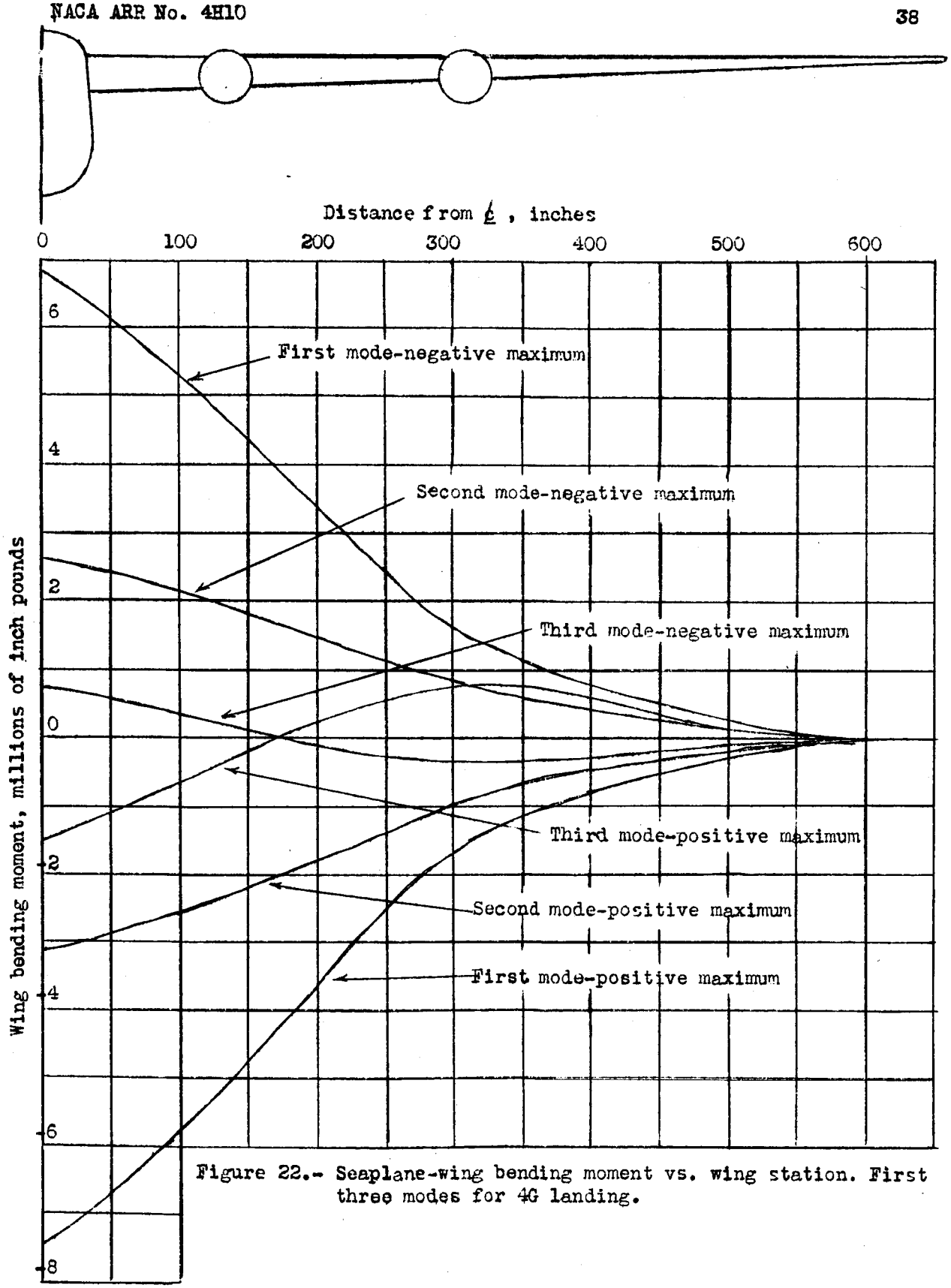

Figure 22.- Seaplane-wing bending moment vs. wing station. First three modes for 4G landing.

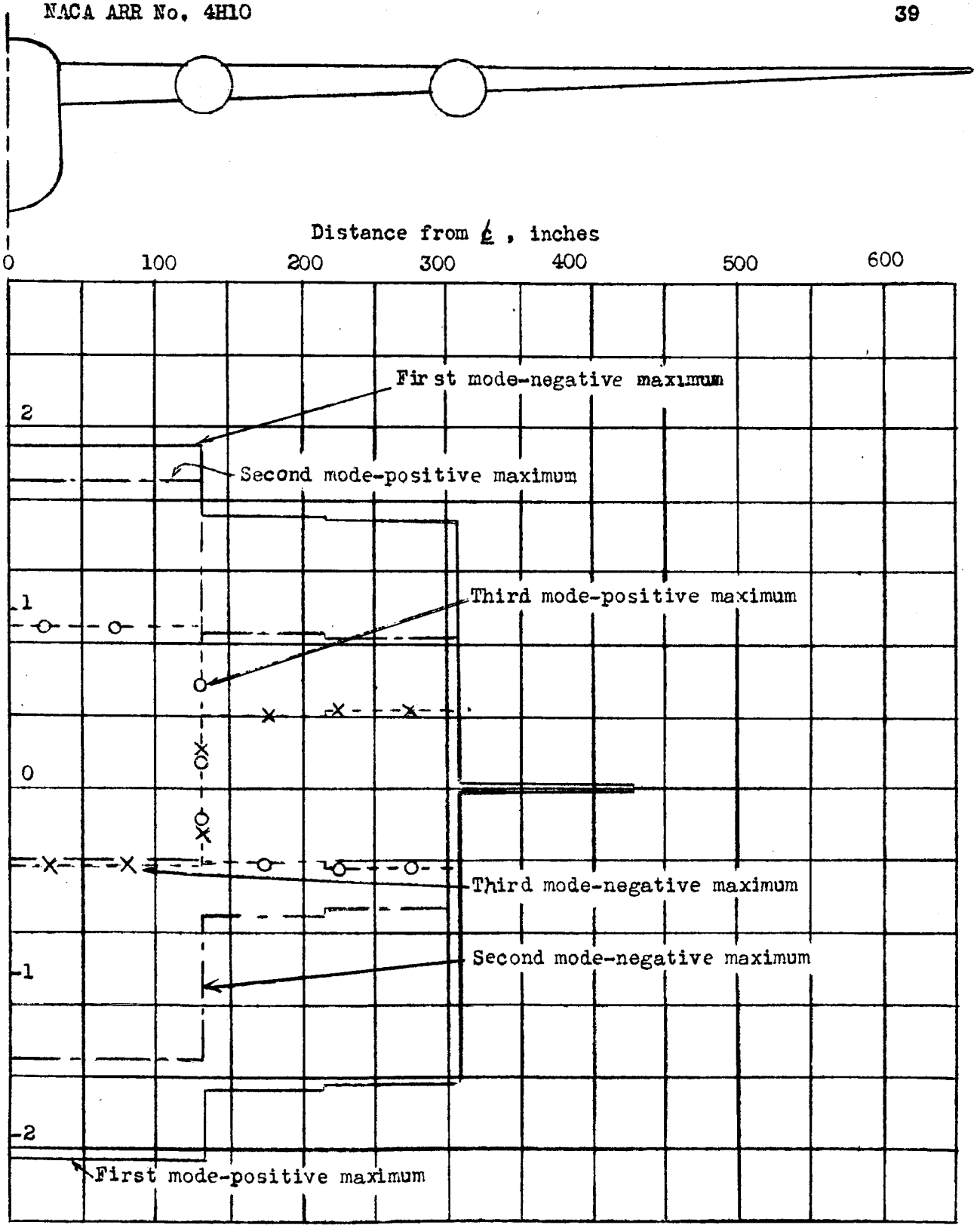

Figure 23.- Seaplane-wing torsional moment vs. wing station. First three modes for 4G landing.

check. Damping has the effect of reducing the amplitudes and coupling the modes.

Coupling between the motion of the structure and the external force is neglected in this discussion; however, this assumption is also subject to experimental check.

The methods discussed here are not universally applicable to all types of transient problems, and should be used with discretion. For example, appendix III discusses the case of a simple beam subjected to a unit impulse applied at the center. In this case, the method is not applicable, since reference to equations (III-11) and (III-13) shows that the series describing the moment and shear does not converge. However, in practical problems, the applied forces do not behave like the impulse type, but rather behave like the step type. In this case, reference to equations (III-10) and (III-12) shows that the series describing the moment converges, whereas the series describing the shear does not converge when maximum values are added regardless of sign. In the case of the procedure discussed here, convergence of the series describing the moment and shear is dependent upon diminishing values of $\phi_F^{(j)}$. This is assured because of the characteristic taper of the airplane wing from center line to wing tip, and because $\phi_F^{(j)}$ is measured at the inboard side of the wedge in its region of greatest mass per unit length. These limitations regarding the convergence of the series apply even more so if one attempts to predict the local accelerations in the structures. This aspect of the problem becomes significant when evaluating the dynamic stresses on the attachments of small localized masses. It is not possible to formulate at this stage a general rule as to how many modes should be taken, and each application of the procedure will present a different problem depending upon the mode shapes and frequencies of the wing.

In the landplane case, the position of the landing gear leg has an important effect upon the wing dynamic loads during impact. For example, if the leg intersects a nodal line for one of the modes, that particular mode is not excited. The effect of various landing gear positions on the stresses may be readily studied by these methods.

In studying the present day large aircraft with conventional wings, it appears as though wing dynamic loads will

produce torsional moments inboard of the nacelles which, aggravated by the overhanging engines, may be critical in severe impact. The design of the nacelle carry through structure in bending may be controlled by dynamic loads, and the possibility of critical wing bending stresses is not precluded in very large aircraft.

A comparison between the landplane and flying boat examples given in sections 12 and 13 shows that the wing dynamic loads in the flying boat are more severe than in the case of the landplane. This is attributed to two causes:

(a) In the case of the second mode in the landplane example, the drag force actually has a relieving effect on the stresses produced by the vertical force.

(b) In the case of all modes $\phi_F^{(j)}$ at the center line is greater than $\phi_F^{(j)}$ at station 1 - that is, the forces introduced at the landing gear are applied nearer to the nodal lines than forces introduced through the hull at the airplane center line.

The present work is of a preliminary nature and many questions are left for further investigation. It is evident that the methods here presented are not restricted to the evaluation of landing loads, since it is possible at least theoretically to handle in the samo way dynamic loads due to gun recoil and "flak." It must be remembered, however, that in flight the aerodynamic forces become of primary importance and cannot be generally neglected. This is especially true in the determination of dynamic loads due to gusts in which case the flutter characteristics of the airplane must have a preponderant effect. It must also be kept in mind that the possibility that the representation of the transient motion as a superposition of natural modes is not necessarily the best procedure in all cases. Considering the dynamic stresses from the standpoint of wave propagation in the elastic system might turn out to be a more direct and significant viewpoint in the case of high frequency transients. This viewpoint also eliminates the convergence difficulties mentioned above in connection with the determination of local accelerations. Another case where natural modes lose their significance is that of resonance between loosely coupled parts of the structure, in which case the vibrational energy at one location is gradually transferred to another.

Examples shown in the present work are limited to the wing structure under the assumptions of a symmetric landing. Such a landing condition is exceptional. For a landplane the degree to which the unsymmetric modes are excited by an unsymmetric landing depends a great deal on the time interval between the instant at which the left and right wheel enter in contact with the ground. Statistical data on this time interval can only be obtained by flight testing. No example has been presented of an application of the procedure to the evaluation of landing loads in the fuselage and tail. However, the same methods are directly applicable to this case, provided the natural modes of the fuselage and tail have been determined. Data obtained during landing tests of flying boats have shown that modes of the fuselage and tail are excited and result in a "tail whip" effect causing considerable dynamic overstress in the tail and aft portion of fuselage.

Bureau of Aeronautics,
U. S. Navy Department,
Washington, D. C., August 10, 1944.

APPENDIX I

GENERAL MATHEMATICAL THEORY OF TRANSIENTS IN AN UNDAMPED ELASTIC STRUCTURE

The general transient theory of linear systems with lumped or distributed parameters is well known and has been extensively developed in the case of electrical network theory (references 2 and 3). The problem of transients in airplane structures is identical in its mathematical form. In an elastic system with distributed parameters there is a space as well as a time variation in the variables. The problem may be considered with two viewpoints. The motion may be considered to be made up of a series of traveling waves, or it may be considered to be made up of a superposition of natural oscillations, in which case to be rigorous, an infinite number is required. The airplane structures problem is treated here from the standpoint of a superposition of natural oscillations.

In a transient problem of this type where maximum values occur very soon after the motion starts, the effect of damping may be justifiably neglected. The motion of an undamped elastic system may be shown to be composed of a superposition of normal modes which are orthogonal. The airplane structure vibrates in a series of normal modes when excited by a random impulse as is the case of any elastic system. These normal modes are each characterized by a certain mode shape and a certain frequency. For the airplane they are composed of coupled oscillations of the wing, fuselage, and empennage system. These calculated mode shapes and frequencies may be obtained from a ground vibration survey of the airplane.

If each normal mode shape is considered to be represented by the space function $\Phi^{(i)}$ the displacement of any point of the structure at any time may be written as

$$z = \sum_{i=o}^{n} \Phi^{(i)} q_i \qquad (I-1)$$

where n modes are considered, and where the q_i terms are regarded as generalized coordinates.

The kinetic energy of the structure is

$$T = \frac{1}{2}\int\left\{\sum_{i=o}^{n} \phi(i)\ \dot{q}_i\right\}^2 dm \qquad (I-2)$$

Considering the jth generalized coordinate, and the orthogonality condition, the following equation may be written

$$\frac{d}{dt}\left(\frac{\partial T}{\partial \dot{q}_j}\right) = \ddot{q}_j \int\left[\phi^{(j)}\right]^2 dm = M_j\ \ddot{q}_j \qquad (I-3)$$

where

$$M_j = \int\left[\phi^{(j)}\right]^2 dm$$

The potential energy of the structure is

$$U = \frac{1}{2}\sum_{i=o}^{n} M_i\ \omega_i^2\ q_i^2 \qquad (I-4)$$

Considering the jth generalized coordinate, write

$$\frac{\partial U}{\partial q_j} = M_j\ \omega_j^2\ q_j \qquad (I-5)$$

By Lagrange's equation

$$M_j\ \ddot{q}_j + M_j\ \omega_j^2\ q_j = Q_j \qquad (I-6)$$

where Q_j is the generalized force corresponding to the jth mode, and is evaluated by virtual work principles.

If δW_j is the virtual work produced when all the external forces are allowed to move through displacements corresponding to a virtual displacement δq_j, then the generalized force Q_j is defined by

$$Q_j = \frac{\delta W_j}{\delta q_j} \tag{I-7}$$

The complete motion of the structure is then defined by a series of differential equations of the form

$$\ddot{q}_j + \omega_j^2 q_j = \frac{Q_j}{M_j}$$

where the form of the right-hand side is dependent upon the character of the applied forces.

In general, the aerodynamic applied forces on an airplane structure vary with deflection, velocity, and acceleration of the structure, and the landing reactions vary with time in a manner which is determined by experiment. In the case where the external forces are landing reactions assumed to be given functions of time, the equations governing the response are

$$\ddot{q}_j + \omega_j^2 q_j = \frac{Q_j(t)}{M_j} \tag{I-8}$$

This is the differential equation for the undamped motion of a simple oscillator of mass M_j and natural frequency ω_j, which is under the influence of an arbitrary forcing impulse $Q_j(t)$.

If $Q_j(t)$ is a unit step function $1(t)$, the response q_j which is called the indicial admittance (references 3 and 4) is

$$A(t) = \frac{1}{M_j \omega_j^2} (1 - \cos \omega_j t)\, 1(t) \tag{I-9}$$

The response q_j to any arbitrary forcing impulse $Q_j(\tau)$ may be written by the superposition theorem as

$$q_j = \frac{1}{M_j \omega_j} \int_0^t Q_j(\tau) \sin \omega_j (t - \tau) \, d\tau \qquad \text{(I-10)}$$

τ is a variable of integration.

When this integration with respect to τ is carried out between the limits 0 and t, a function of time results which is the time history of the deformation of the jth mode. The stress at any point in the structure in the jth mode is proportional to the deformation of the jth mode.

$$s^{(j)} = A^{(j)} q_j = \frac{A^{(j)}}{M_j \omega_j} \int_0^t Q_j(\tau) \sin \omega_j (t - \tau) d\tau \qquad \text{(I-11)}$$

When the constant $A^{(j)}$ is properly chosen, equation (I-11) yields the stress time history of some particular point in the structure caused by the deformation of the jth mode. The stress $s_k^{(j)}$ in the jth mode at the kth wing station may be written as

$$s_k^{(j)} = A_k^{(j)} q_j \qquad \text{(I-12)}$$

The total stress at the kth wing station for n modes is obtained by superposition as

$$s_k = \sum_{i=1}^{n} A_k^{(i)} q_i \qquad \text{(I-13)}$$

Note on the Computation of M_j for the Wing

From equation (I-3)

$$M_j = \int \left[\phi^{(j)}\right]^2 dm$$

For the case of the wing, the mode shape is conveniently described by considering the wing deformation to be made up of a bending of the elastic axis, and a twisting about the elastic axis. Considering the wing to be divided into k spanwise stations, the normal function describing any point on the chord of the kth station is (see fig. I-1)

$$\phi_k^{(j)} = h_k^{(j)} + x\,\alpha_k^{(j)} \tag{I-14}$$

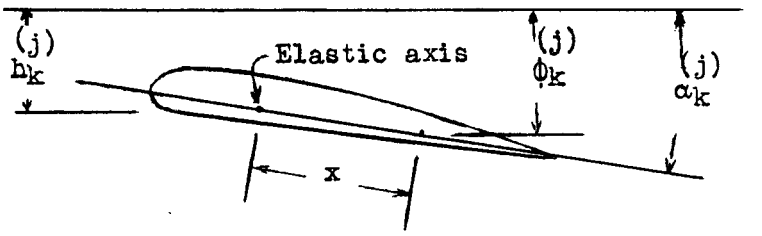

Figure I-1

In figure I-1 positive bending deflections are downward and positive pitching deflections are stalling.

Using equations (I-3) and (I-12), the following equations may be written

$$M_j = \int \left[\phi^{(j)}\right]^2 dm$$

$$M_j = \sum^{k} \left\{\left[h_k^{(j)}\right]^2 m_k + \left[\alpha_k^{(j)}\right]^2 I_k + 2h_k^{(j)}\,\alpha_k^{(j)}\,S_k\right\} \tag{I-15}$$

Note on the Computation of the Generalized Force Q_j

From equation (I-7)

$$Q_j = \frac{\delta W}{\delta q_j}$$

If the external force $F(t)$ is a landing reaction considered to be applied at one point to the wing structure, the virtual work may be written as

$$\delta W = F(t)\ \delta z_F$$

where z_F is the value of z in the direction of the applied force evaluated at the point F, the point of application of the landing force.

From equation (I-1)

$$z = \phi^{(1)}\ q_1 + \phi^{(2)}\ q_2 + \ldots \phi^{(n)}\ q_n$$

hence

$$\delta W = F(t) \left\{ \phi_F^{(1)}\ \delta q_1 + \phi_F^{(2)}\ \delta q_2 + \ldots \phi_F^{(n)}\ \delta q_n \right\}$$

where $\phi_F^{(j)}$ is the normal function evaluated at the point of application of the force F.

Then

$$Q_j = \frac{\delta W}{\delta q_j} = \phi_F^{(j)}\ F(t) \qquad \text{(I-16)}$$

The factor $\phi_F^{(j)}$ is a measure of the contribution of the external force to the generalized force in the jth mode.

APPENDIX II

ANALYSIS OF THE MOTION OF A SYSTEM CONSISTING OF TWO SPRING-CONNECTED MASSES EXCITED BY AN ARBITRARY FORCE

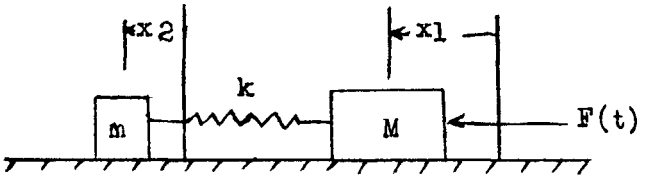

Figure II-1

It is shown below that the motions of the mass m are given by a superposition of the motion of the center of gravity of the system, and the motion of a simple oscillator which will be defined. Denote by x_1, x_2 the coordinates of the masses M and m.

The differential equations defining the motion are:

$$M\ddot{x}_1 + k(x_1 - x_2) = F(t) \qquad (II-1)$$

$$m\ddot{x}_2 - k(x_1 - x_2) = 0 \qquad (II-2)$$

The motion of the center of gravity of the system is determined first. Adding equations (II-1) and (II-2) gives

$$M\ddot{x}_1 + m\ddot{x}_2 = F(t)$$

Let q_0 be the displacement of the center of gravity of the system

$$mx_2 + Mx_1 = (M + m)\,q_0$$

and

$$m\ddot{x}_2 + M\ddot{x}_1 = (M + m)\,\ddot{q}$$

Hence

$$(M + m)\ \ddot{q}_o = F(t)$$

is the differential equation defining the motion of the center of gravity of the system.

The motion of the mass m relative to the center of gravity of the system is determined next.

Multiplying equations (II-1) and (II-2) by m and M, respectively, and subtracting, the following equation is obtained

$$Mm(\ddot{x}_1 - \ddot{x}_2) + k(M + m)(x_1 - x_2) = mF(t)$$

and substituting

$$q_1 = \frac{M}{M + m}\ (x_1 - x_2)$$

which represents the motion of m relative to the center of gravity; the differential equation may be rewritten as

$$\frac{m}{M}\ (m + M)\ \ddot{q}_1 + k\left(\frac{m + M}{M}\right)^2 q_1 = \frac{m}{M}\ F(t) \qquad \text{(II-4)}$$

Let

$$M_1 = \frac{m}{M}\ (m + M)$$

$$M_1\omega_1^{\,2} = k\left(\frac{m + M}{M}\right)^2$$

$$Q_1(t) = \frac{m}{M}\ F(t)$$

and write

$$M_1\ \ddot{q}_1 + M_1\omega_1^{\,2}\ q_1 = Q_1(t) \qquad \text{(II-5)}$$

This is the differential equation defining the motion of m relative to the center of gravity of the system. It is also

the differential equation for a simple oscillator. (See fig. II-2.)

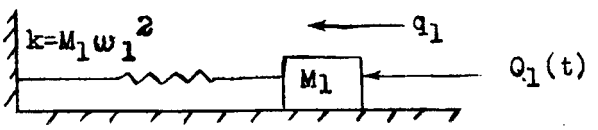

Figure II-2

The actual displacements x_1 and x_2 may be derived by solving for x_1, x_2.

From the relations

$$mx_2 + Mx_1 = (M + m)\, q_0$$

$$(x_1 - x_2)\,\frac{M}{M + m} = q_1$$

may be found

$$x_1 = q_0 + \frac{m}{M}\, q_1$$

$$x_2 = q_0 - q_1$$

The motion may be considered as the superposition of two configurations, one defined by q_0, a rigid motion of the system, the other defined by q_1 represents a configuration in which the center of gravity remains fixed while the masses M and m move in opposite phase with amplitudes inversely proportional to their masses. The equivalent system of figure II-2 represents the motion in the latter configuration. It will be noted that the generalized mass M_1 may be derived quite simply by considering the kinetic energy T in the corresponding configuration

$$T = \frac{1}{2}\, m\dot{q}_1^{\,2} + \frac{1}{2}\, M\left(\frac{m}{M}\right)^2 \dot{q}_1^{\,2}$$

or

$$T = \frac{1}{2}\frac{m}{M}(m + M)\ \dot{q}_1^2$$

Equating this to the kinetic energy of the equivalent oscillation

$$T = \frac{1}{2} M_1\ \dot{q}_1^2$$

there is found

$$M_1 = \frac{m}{M}(m + M)$$

Similarly $Q_1(t)$ may be derived by equating the work done by $F(t)$ in the corresponding configuration and the work done by Q_1 in the equivalent system.

$$Q_1(t)\ q_1 = F(t)\ \frac{m}{M}\ q_1$$

Hence

$$Q_1(t) = \frac{m}{M}\ F(t)$$

APPENDIX III

TRANSIENTS IN A PRISMATIC BEAM SIMPLY SUPPORTED AT THE ENDS WITH A FORCE APPLIED AT THE CENTER

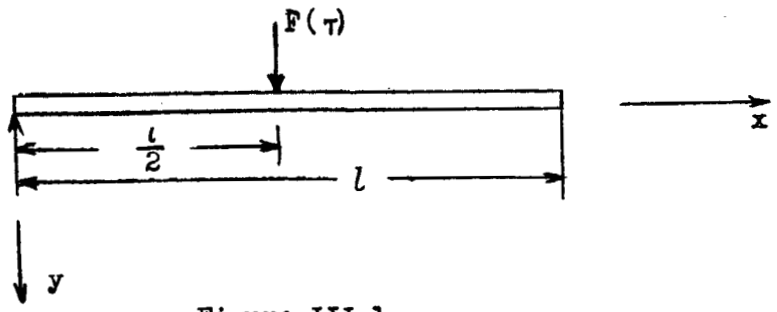

Figure III-1

The natural mode shapes and frequencies of a simply supported beam with constant cross section may be shown to be:

$$\phi^{(i)} = \sin \frac{i\pi x}{l} \tag{III-1}$$

$$\omega_i = i^2 \pi^2 \sqrt{\frac{EI}{\rho A l^4}} \tag{III-2}$$

where

E modulus of elasticity

I moment of inertia

ρ mass per unit volume

A cross-sectional area

l length

From equation (I-1) of appendix I, the displacement of any point on the beam may be written as

$$y = \sum_{i=o}^{\infty} \phi^{(i)} q_i = \sum_{i=1}^{\infty} \sin \frac{i\pi x}{l} q_i \tag{III-3}$$

From equation (I-10) of appendix I, the generalized coordinate q_i is expressed by

$$q_i = \frac{1}{M_i \omega_i} \int_0^t Q_i(\tau) \sin \omega_i (t - \tau) \, d\tau \tag{III-4}$$

where

$$M_i = \int \left[\phi^{(i)}\right]^2 dm = \rho A \int_0^l \sin^2 \frac{i\pi x}{l} \, dx = \frac{l\rho A}{2} \tag{III-5}$$

and

$$Q_i(\tau) = \Phi_F^{(i)} F(\tau) = \sin \frac{i\pi}{2} F(\tau) \qquad \text{(III-6)}$$

Substituting equations (III-4), (III-5), and (III-6) into equation (III-3) yields,

$$y = \frac{2}{l\rho A} \sum_{i=1}^{\infty} \frac{1}{\omega_i} \sin \frac{i\pi}{2} \sin \frac{i\pi x}{l} \int_0^t F(\tau) \sin \omega_i (t - \tau) d\tau \qquad \text{(III-7)}$$

When $F(\tau)$ is a unit step, the response is:-

$$y = \frac{2}{l\rho A} \sum_{i=1}^{\infty} \frac{1}{\omega_i^2} \sin \frac{i\pi}{2} \sin \frac{i\pi x}{l} (1 - \cos \omega_i t) \qquad \text{(III-8)}$$

When $F(\tau)$ is a unit impulse [1], the response is obtained by a time differentiation of equation (III-8). The response to a unit impulse is:

$$y = \frac{2}{l\rho A} \sum_{i=1}^{\infty} \frac{1}{\omega_i} \sin \frac{i\pi}{2} \sin \frac{i\pi x}{l} \sin \omega_i t \qquad \text{(III-9)}$$

Since $M = -EI \frac{\partial^2 y}{\partial x^2}$, the moment in the beam at any time after being subjected to a unit step force is,

$$M = \frac{2l}{\pi^2} \sum_{i=1}^{\infty} \frac{1}{i^2} \sin \frac{i\pi}{2} \sin \frac{i\pi x}{l} (1 - \cos \omega_i t) \qquad \text{(III-10)}$$

The moment in the beam at any time after being subjected to a unit impulse is,

---

[1] A unit impulse is an infinite force applied during a vanishingly small interval of time in such a way that the time integral $\int F(\tau)\, d\tau = 1$ (reference 4).

$$M = \frac{2}{l}\sqrt{\frac{EI}{\rho A}}\sum_{i=1}^{\infty}\sin\frac{i\pi}{2}\sin\frac{i\pi x}{l}\sin\omega_i t \qquad \text{(III-11)}$$

The shear in the beam at any time after being subjected to a unit step force is,

$$\frac{\partial M}{\partial x} = \frac{2}{\pi}\sum_{i=1}^{\infty}\frac{1}{i}\sin\frac{i\pi}{2}\cos\frac{i\pi x}{l}(1 - \cos\omega_i t) \qquad \text{(III-12)}$$

The shear in the beam at any time after being subjected to a unit impulse is,

$$\frac{\partial M}{\partial x} = \frac{2\pi}{l^2}\sqrt{\frac{EI}{\rho A}}\sum_{i=1}^{\infty} i\sin\frac{i\pi}{2}\cos\frac{i\pi x}{l}\sin\omega_i t \qquad \text{(III-13)}$$

A study of equations (III-10), (III-11), (III-12), and (III-13) indicates the shortcomings of the procedure when adding contributions of each of the modes to moment and shear for a simple prismatic beam with a force at the center. This is illustrated in table III-1. Limitations of a similar nature are encountered in all problems where the motion is described as a superposition of modes.

TABLE III-1

UNIT STEP		UNIT IMPULSE	
	Percent of 1st mode		Percent of 1st mode
Moment		Moment	
1st mode	100	1st mode	100
2nd mode	11.1	2nd mode	100
3rd mode	4	3rd mode	100
4th mode	2.04	4th mode	100
Shear		Shear	
1st mode	100	1st mode	100
2nd mode	33.3	2nd mode	300
3rd mode	20	3rd mode	500
4th mode	14.3	4th mode	700

REFERENCES

1. Biot, M. A.: Analytical and Experimental Methods in Engineering Seismology. Trans. Am. Soc. of Civil Eng., vol. 108, 1943, p. 365.

2. Gardner, Murray F., and Barnes, John L.: Transients in Linear Systems. John Wiley & Sons, Inc., 1942.

3. Bush, Vannevar: Operational Circuit Analysis. John Wiley & Sons, Inc., 1929.

4. von Kármán, Th., and Biot, Maurice A.: Mathematical Methods in Engineering. McGraw Hill Book Co., Inc., 1940.

BIBLIOGRAPHY

Fairthorne, R. A.: The Effects of Landing Shock on Wing and Undercarriage Deflection. R. & M. No. 1877, British A.R.C., 1939.